



# 3 *Image Enhancement in the Spatial Domain*

It makes all the difference whether one sees darkness  
through the light or brightness through the shadows.

*David Lindsay*

## *Preview*

The principal objective of enhancement is to process an image so that the result is more suitable than the original image for a specific application. The word *specific* is important, because it establishes at the outset that the techniques discussed in this chapter are very much problem oriented. Thus, for example, a method that is quite useful for enhancing X-ray images may not necessarily be the best approach for enhancing pictures of Mars transmitted by a space probe. Regardless of the method used, however, image enhancement is one of the most interesting and visually appealing areas of image processing.

Image enhancement approaches fall into two broad categories: spatial domain methods and frequency domain methods. The term *spatial domain* refers to the image plane itself, and approaches in this category are based on direct manipulation of pixels in an image. *Frequency domain* processing techniques are based on modifying the Fourier transform of an image. Spatial methods are covered in this chapter, and frequency domain enhancement is discussed in Chapter 4. Enhancement techniques based on various combinations of methods from these two categories are not unusual. We note also that many of the fundamental techniques introduced in this chapter in the context of enhancement are used in subsequent chapters for a variety of other image processing applications.

There is no general theory of image enhancement. When an image is processed for visual interpretation, the viewer is the ultimate judge of how well

a particular method works. Visual evaluation of image quality is a highly subjective process, thus making the definition of a “good image” an elusive standard by which to compare algorithm performance. When the problem is one of processing images for machine perception, the evaluation task is somewhat easier. For example, in dealing with a character recognition application, and leaving aside other issues such as computational requirements, the best image processing method would be the one yielding the best machine recognition results. However, even in situations when a clear-cut criterion of performance can be imposed on the problem, a certain amount of trial and error usually is required before a particular image enhancement approach is selected.

### 3.1 Background

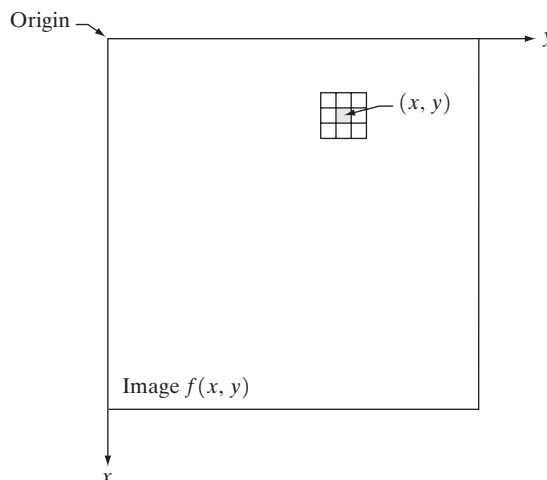
As indicated previously, the term *spatial domain* refers to the aggregate of pixels composing an image. Spatial domain methods are procedures that operate directly on these pixels. Spatial domain processes will be denoted by the expression

$$g(x, y) = T[f(x, y)] \quad (3.1-1)$$

where  $f(x, y)$  is the input image,  $g(x, y)$  is the processed image, and  $T$  is an operator on  $f$ , defined over some neighborhood of  $(x, y)$ . In addition,  $T$  can operate on a *set* of input images, such as performing the pixel-by-pixel sum of  $K$  images for noise reduction, as discussed in Section 3.4.2.

The principal approach in defining a neighborhood about a point  $(x, y)$  is to use a square or rectangular subimage area centered at  $(x, y)$ , as Fig. 3.1 shows. The center of the subimage is moved from pixel to pixel starting, say, at the top left corner. The operator  $T$  is applied at each location  $(x, y)$  to yield the output,  $g$ , at that location. The process utilizes only the pixels in the area of the image spanned by the neighborhood. Although other neighborhood shapes, such as ap-

**FIGURE 3.1** A  $3 \times 3$  neighborhood about a point  $(x, y)$  in an image.



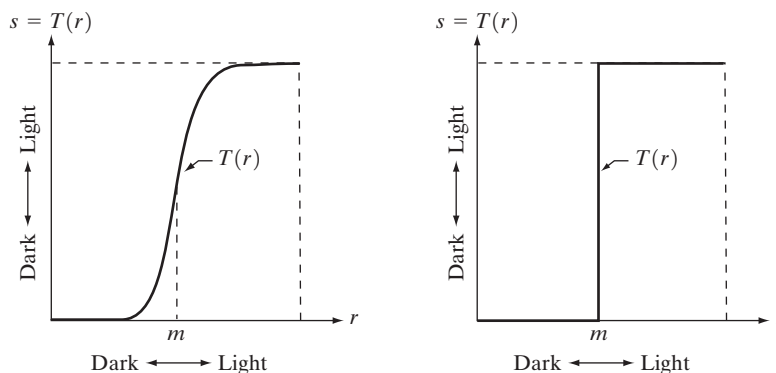
proximations to a circle, sometimes are used, square and rectangular arrays are by far the most predominant because of their ease of implementation.

The simplest form of  $T$  is when the neighborhood is of size  $1 \times 1$  (that is, a single pixel). In this case,  $g$  depends only on the value of  $f$  at  $(x, y)$ , and  $T$  becomes a *gray-level* (also called an *intensity* or *mapping*) *transformation function* of the form

$$s = T(r) \quad (3.1-2)$$

where, for simplicity in notation,  $r$  and  $s$  are variables denoting, respectively, the gray level of  $f(x, y)$  and  $g(x, y)$  at any point  $(x, y)$ . For example, if  $T(r)$  has the form shown in Fig. 3.2(a), the effect of this transformation would be to produce an image of higher contrast than the original by darkening the levels below  $m$  and brightening the levels above  $m$  in the original image. In this technique, known as *contrast stretching*, the values of  $r$  below  $m$  are compressed by the transformation function into a narrow range of  $s$ , toward black. The opposite effect takes place for values of  $r$  above  $m$ . In the limiting case shown in Fig. 3.2(b),  $T(r)$  produces a two-level (binary) image. A mapping of this form is called a *thresholding* function. Some fairly simple, yet powerful, processing approaches can be formulated with gray-level transformations. Because enhancement at any point in an image depends only on the gray level at that point, techniques in this category often are referred to as *point processing*.

Larger neighborhoods allow considerably more flexibility. The general approach is to use a function of the values of  $f$  in a predefined neighborhood of  $(x, y)$  to determine the value of  $g$  at  $(x, y)$ . One of the principal approaches in this formulation is based on the use of so-called *masks* (also referred to as *filters*, *kernels*, *templates*, or *windows*). Basically, a mask is a small (say,  $3 \times 3$ ) 2-D array, such as the one shown in Fig. 3.1, in which the values of the mask coefficients determine the nature of the process, such as image sharpening. Enhancement techniques based on this type of approach often are referred to as *mask processing* or *filtering*. These concepts are discussed in Section 3.5.



**a b**  
**FIGURE 3.2** Gray-level transformation functions for contrast enhancement.

### 3.2 Some Basic Gray Level Transformations

We begin the study of image enhancement techniques by discussing gray-level transformation functions. These are among the simplest of all image enhancement techniques. The values of pixels, before and after processing, will be denoted by  $r$  and  $s$ , respectively. As indicated in the previous section, these values are related by an expression of the form  $s = T(r)$ , where  $T$  is a transformation that maps a pixel value  $r$  into a pixel value  $s$ . Since we are dealing with digital quantities, values of the transformation function typically are stored in a one-dimensional array and the mappings from  $r$  to  $s$  are implemented via table lookups. For an 8-bit environment, a lookup table containing the values of  $T$  will have 256 entries.

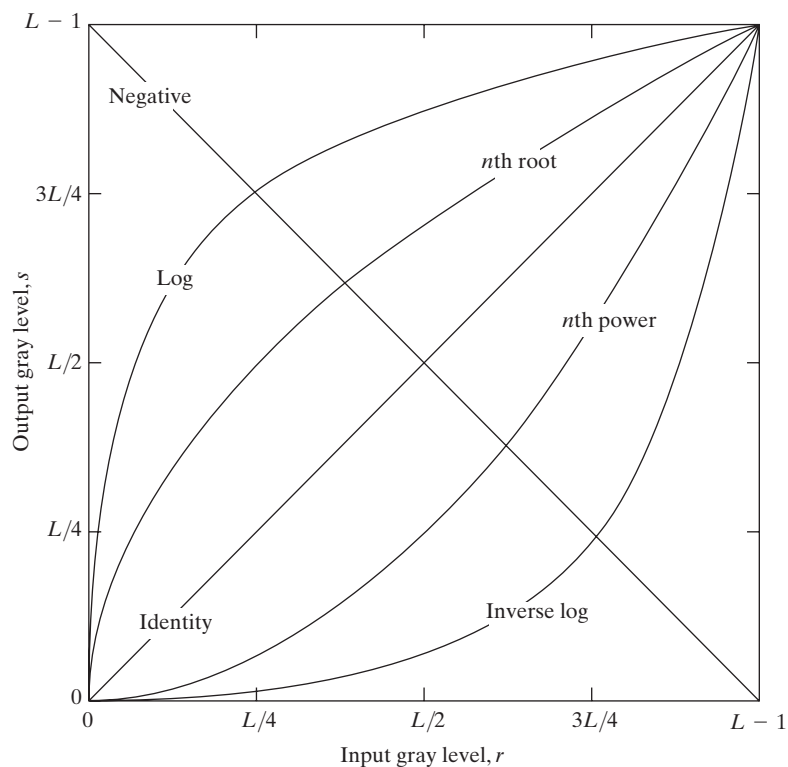
As an introduction to gray-level transformations, consider Fig. 3.3, which shows three basic types of functions used frequently for image enhancement: linear (negative and identity transformations), logarithmic (log and inverse-log transformations), and power-law ( $n$ th power and  $n$ th root transformations). The identity function is the trivial case in which output intensities are identical to input intensities. It is included in the graph only for completeness.

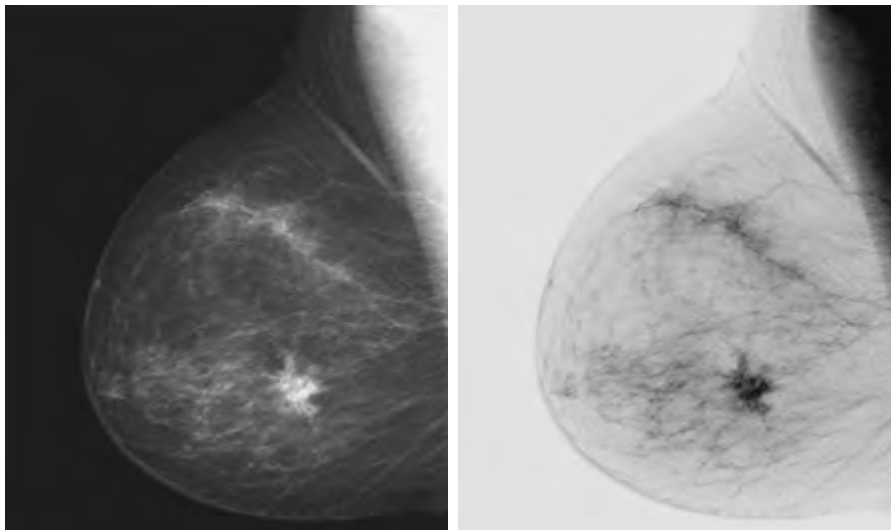
#### 3.2.1 Image Negatives

The negative of an image with gray levels in the range  $[0, L - 1]$  is obtained by using the negative transformation shown in Fig. 3.3, which is given by the expression

$$s = L - 1 - r. \quad (3.2-1)$$

**FIGURE 3.3** Some basic gray-level transformation functions used for image enhancement.





**a b**  
**FIGURE 3.4**  
 (a) Original digital mammogram.  
 (b) Negative image obtained using the negative transformation in Eq. (3.2-1).  
 (Courtesy of G.E. Medical Systems.)

Reversing the intensity levels of an image in this manner produces the equivalent of a photographic negative. This type of processing is particularly suited for enhancing white or gray detail embedded in dark regions of an image, especially when the black areas are dominant in size. An example is shown in Fig. 3.4. The original image is a digital mammogram showing a small lesion. In spite of the fact that the visual content is the same in both images, note how much easier it is to analyze the breast tissue in the negative image in this particular case.

### 3.2.2 Log Transformations

The general form of the log transformation shown in Fig. 3.3 is

$$s = c \log(1 + r) \quad (3.2-2)$$

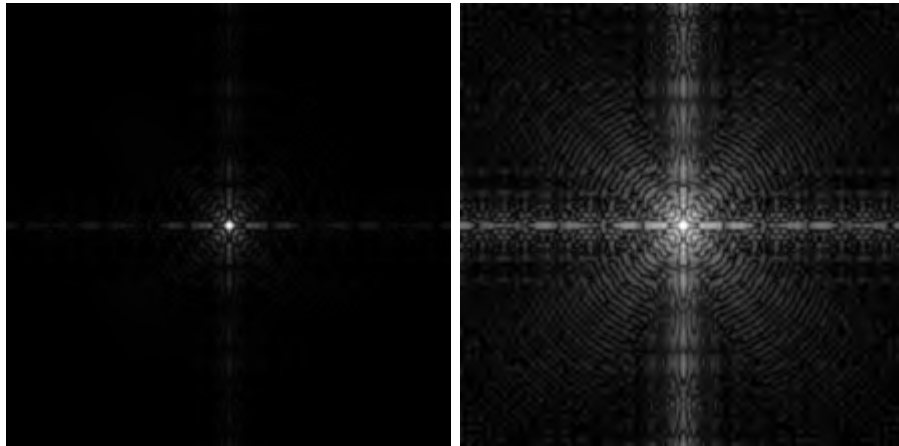
where  $c$  is a constant, and it is assumed that  $r \geq 0$ . The shape of the log curve in Fig. 3.3 shows that this transformation maps a narrow range of low gray-level values in the input image into a wider range of output levels. The opposite is true of higher values of input levels. We would use a transformation of this type to expand the values of dark pixels in an image while compressing the higher-level values. The opposite is true of the inverse log transformation.

Any curve having the general shape of the log functions shown in Fig. 3.3 would accomplish this spreading/compressing of gray levels in an image. In fact, the power-law transformations discussed in the next section are much more versatile for this purpose than the log transformation. However, the log function has the important characteristic that it compresses the dynamic range of images with large variations in pixel values. A classic illustration of an application in which pixel values have a large dynamic range is the Fourier spectrum, which will be discussed in Chapter 4. At the moment, we are concerned only with the image characteristics of spectra. It is not unusual to encounter spectrum values

a b

**FIGURE 3.5**

(a) Fourier spectrum.  
 (b) Result of applying the log transformation given in Eq. (3.2-2) with  $c = 1$ .



that range from 0 to  $10^6$  or higher. While processing numbers such as these presents no problems for a computer, image display systems generally will not be able to reproduce faithfully such a wide range of intensity values. The net effect is that a significant degree of detail will be lost in the display of a typical Fourier spectrum.

As an illustration of log transformations, Fig. 3.5(a) shows a Fourier spectrum with values in the range 0 to  $1.5 \times 10^6$ . When these values are scaled linearly for display in an 8-bit system, the brightest pixels will dominate the display, at the expense of lower (and just as important) values of the spectrum. The effect of this dominance is illustrated vividly by the relatively small area of the image in Fig. 3.5(a) that is not perceived as black. If, instead of displaying the values in this manner, we first apply Eq. (3.2-2) (with  $c = 1$  in this case) to the spectrum values, then the range of values of the result become 0 to 6.2, a more manageable number. Figure 3.5(b) shows the result of scaling this new range linearly and displaying the spectrum in the same 8-bit display. The wealth of detail visible in this image as compared to a straight display of the spectrum is evident from these pictures. Most of the Fourier spectra seen in image processing publications have been scaled in just this manner.

### 3.2.3 Power-Law Transformations

Power-law transformations have the basic form

$$s = cr^\gamma \quad (3.2-3)$$

where  $c$  and  $\gamma$  are positive constants. Sometimes Eq. (3.2-3) is written as  $s = c(r + \epsilon)^\gamma$  to account for an offset (that is, a measurable output when the input is zero). However, offsets typically are an issue of display calibration and as a result they are normally ignored in Eq. (3.2-3). Plots of  $s$  versus  $r$  for various values of  $\gamma$  are shown in Fig. 3.6. As in the case of the log transformation, power-law curves with fractional values of  $\gamma$  map a narrow range of dark input values into a wider range of output values, with the opposite being true for high-

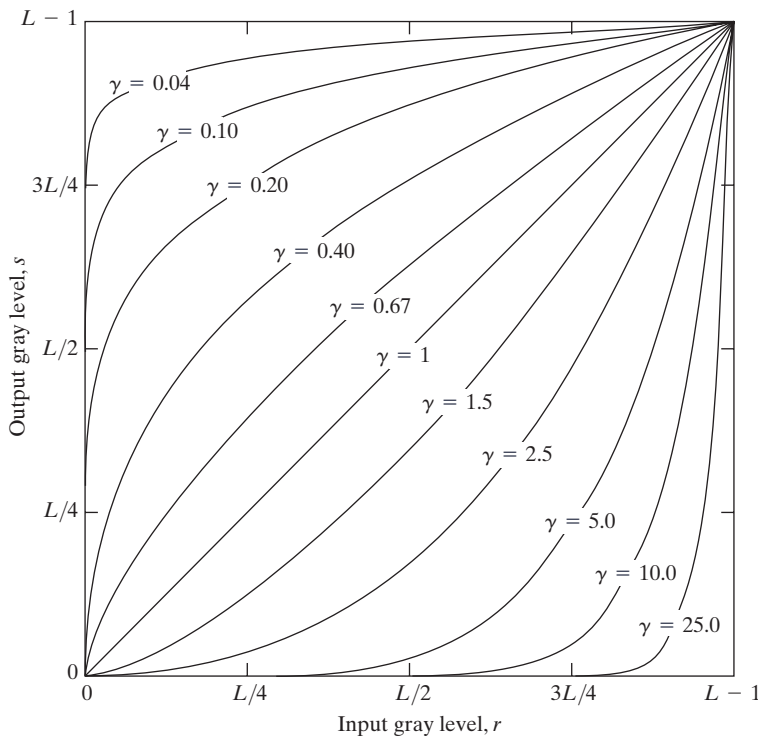


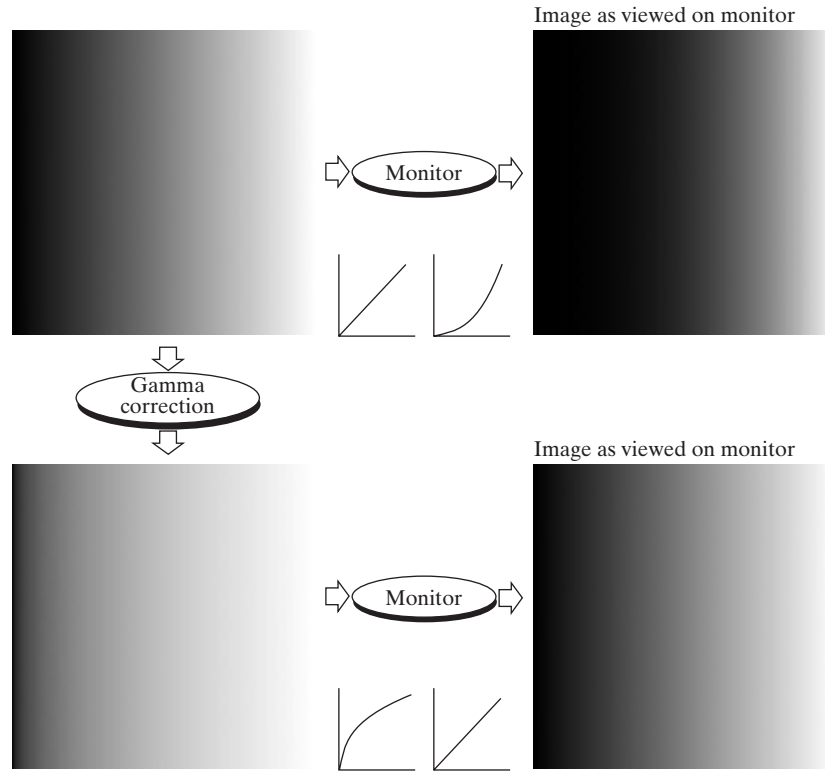
**FIGURE 3.6** Plots of the equation  $s = cr^\gamma$  for various values of  $\gamma$  ( $c = 1$  in all cases).

er values of input levels. Unlike the log function, however, we notice here a family of possible transformation curves obtained simply by varying  $\gamma$ . As expected, we see in Fig. 3.6 that curves generated with values of  $\gamma > 1$  have exactly the opposite effect as those generated with values of  $\gamma < 1$ . Finally, we note that Eq. (3.2-3) reduces to the identity transformation when  $c = \gamma = 1$ .

A variety of devices used for image capture, printing, and display respond according to a power law. By convention, the exponent in the power-law equation is referred to as *gamma* [hence our use of this symbol in Eq. (3.2-3)]. The process used to correct this power-law response phenomena is called *gamma correction*. For example, cathode ray tube (CRT) devices have an intensity-to-voltage response that is a power function, with exponents varying from approximately 1.8 to 2.5. With reference to the curve for  $\gamma = 2.5$  in Fig. 3.6, we see that such display systems would tend to produce images that are darker than intended. This effect is illustrated in Fig. 3.7. Figure 3.7(a) shows a simple gray-scale linear wedge input into a CRT monitor. As expected, the output of the monitor appears darker than the input, as shown in Fig. 3.7(b). Gamma correction in this case is straightforward. All we need to do is preprocess the input image before inputting it into the monitor by performing the transformation  $s = r^{1/2.5} = r^{0.4}$ . The result is shown in Fig. 3.7(c). When input into the same monitor, this gamma-corrected input produces an output that is close in appearance to the original image, as shown in Fig. 3.7(d). A similar analysis would

a b  
c d

**FIGURE 3.7**  
(a) Linear-wedge gray-scale image.  
(b) Response of monitor to linear wedge.  
(c) Gamma-corrected wedge.  
(d) Output of monitor.



apply to other imaging devices such as scanners and printers. The only difference would be the device-dependent value of gamma (Poynton [1996]).

Gamma correction is important if displaying an image accurately on a computer screen is of concern. Images that are not corrected properly can look either bleached out, or, what is more likely, too dark. Trying to reproduce colors accurately also requires some knowledge of gamma correction because varying the value of gamma correction changes not only the brightness, but also the ratios of red to green to blue. Gamma correction has become increasingly important in the past few years, as use of digital images for commercial purposes over the Internet has increased. It is not unusual that images created for a popular Web site will be viewed by millions of people, the majority of whom will have different monitors and/or monitor settings. Some computer systems even have partial gamma correction built in. Also, current image standards do not contain the value of gamma with which an image was created, thus complicating the issue further. Given these constraints, a reasonable approach when storing images in a Web site is to preprocess the images with a gamma that represents an “average” of the types of monitors and computer systems that one expects in the open market at any given point in time.

**EXAMPLE 3.1:**  
Contrast enhancement using power-law transformations.

■ In addition to gamma correction, power-law transformations are useful for general-purpose contrast manipulation. Figure 3.8(a) shows a magnetic resonance (MR) image of an upper thoracic human spine with a fracture dislocation





a b  
c d

**FIGURE 3.8**  
 (a) Magnetic resonance (MR) image of a fractured human spine.  
 (b)–(d) Results of applying the transformation in Eq. (3.2-3) with  $c = 1$  and  $\gamma = 0.6, 0.4,$  and  $0.3,$  respectively. (Original image for this example courtesy of Dr. David R. Pickens, Department of Radiology and Radiological Sciences, Vanderbilt University Medical Center.)

and spinal cord impingement. The fracture is visible near the vertical center of the spine, approximately one-fourth of the way down from the top of the picture. Since the given image is predominantly dark, an expansion of gray levels are desirable. This can be accomplished with a power-law transformation with a fractional exponent. The other images shown in the Figure were obtained by processing Fig. 3.8(a) with the power-law transformation function of Eq. (3.2-3). The values of gamma corresponding to images (b) through (d) are 0.6, 0.4, and 0.3, respectively (the value of  $c$  was 1 in all cases). We note that, as gamma decreased from 0.6 to 0.4, more detail became visible. A further decrease of gamma

to 0.3 enhanced a little more detail in the background, but began to reduce contrast to the point where the image started to have a very slight “washed-out” look, especially in the background. By comparing all results, we see that the best enhancement in terms of contrast and discernable detail was obtained with  $\gamma = 0.4$ . A value of  $\gamma = 0.3$  is an approximate limit below which contrast in this particular image would be reduced to an unacceptable level. ■

**EXAMPLE 3.2:**  
Another illustration of power-law transformations.

■ Figure 3.9(a) shows the opposite problem of Fig. 3.8(a). The image to be enhanced now has a washed-out appearance, indicating that a compression of gray levels is desirable. This can be accomplished with Eq. (3.2-3) using values of  $\gamma$  greater than 1. The results of processing Fig. 3.9(a) with  $\gamma = 3.0$ , 4.0, and 5.0 are shown in Figs. 3.9(b) through (d). Suitable results were obtained with gamma values of 3.0 and 4.0, the latter having a slightly more appealing appearance because it has higher contrast. The result obtained with  $\gamma = 5.0$  has areas that are too dark, in which some detail is lost. The dark region to the left of the main road in the upper left quadrant is an example of such an area. ■

a b  
c d

**FIGURE 3.9**  
(a) Aerial image.  
(b)–(d) Results of applying the transformation in Eq. (3.2-3) with  $c = 1$  and  $\gamma = 3.0$ , 4.0, and 5.0, respectively. (Original image for this example courtesy of NASA.)



### 3.2.4 Piecewise-Linear Transformation Functions

A complementary approach to the methods discussed in the previous three sections is to use piecewise linear functions. The principal advantage of piecewise linear functions over the types of functions we have discussed thus far is that the form of piecewise functions can be arbitrarily complex. In fact, as we will see shortly, a practical implementation of some important transformations can be formulated only as piecewise functions. The principal disadvantage of piecewise functions is that their specification requires considerably more user input.

#### Contrast stretching

One of the simplest piecewise linear functions is a contrast-stretching transformation. Low-contrast images can result from poor illumination, lack of dynamic range in the imaging sensor, or even wrong setting of a lens aperture during image acquisition. The idea behind contrast stretching is to increase the dynamic range of the gray levels in the image being processed.

Figure 3.10(a) shows a typical transformation used for contrast stretching. The locations of points  $(r_1, s_1)$  and  $(r_2, s_2)$  control the shape of the transformation

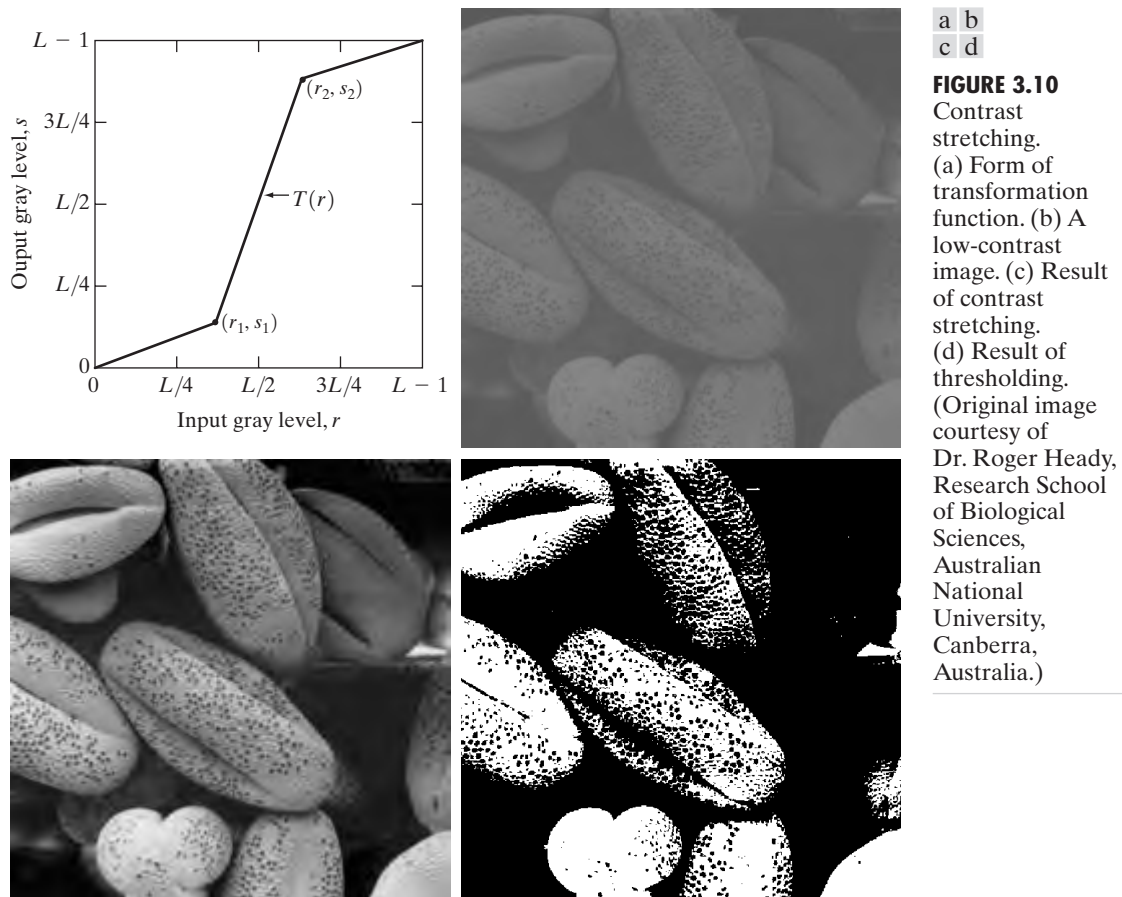


**FIGURE 3.10**  
 Contrast stretching. (a) Form of transformation function. (b) A low-contrast image. (c) Result of contrast stretching. (d) Result of thresholding. (Original image courtesy of Dr. Roger Heady, Research School of Biological Sciences, Australian National University, Canberra, Australia.)

function. If  $r_1 = s_1$  and  $r_2 = s_2$ , the transformation is a linear function that produces no changes in gray levels. If  $r_1 = r_2$ ,  $s_1 = 0$  and  $s_2 = L - 1$ , the transformation becomes a *thresholding function* that creates a binary image, as illustrated in Fig. 3.2(b). Intermediate values of  $(r_1, s_1)$  and  $(r_2, s_2)$  produce various degrees of spread in the gray levels of the output image, thus affecting its contrast. In general,  $r_1 \leq r_2$  and  $s_1 \leq s_2$  is assumed so that the function is single valued and monotonically increasing. This condition preserves the order of gray levels, thus preventing the creation of intensity artifacts in the processed image.

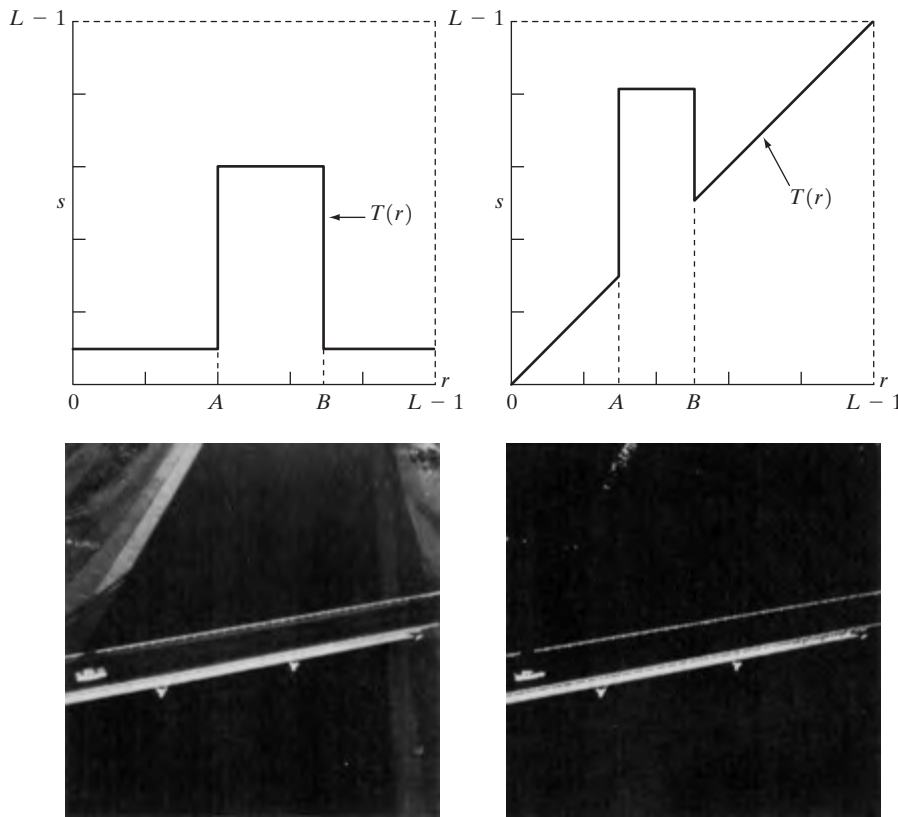
Figure 3.10(b) shows an 8-bit image with low contrast. Fig. 3.10(c) shows the result of contrast stretching, obtained by setting  $(r_1, s_1) = (r_{\min}, 0)$  and  $(r_2, s_2) = (r_{\max}, L - 1)$  where  $r_{\min}$  and  $r_{\max}$  denote the minimum and maximum gray levels in the image, respectively. Thus, the transformation function stretched the levels linearly from their original range to the full range  $[0, L - 1]$ . Finally, Fig. 3.10(d) shows the result of using the thresholding function defined previously, with  $r_1 = r_2 = m$ , the mean gray level in the image. The original image on which these results are based is a scanning electron microscope image of pollen, magnified approximately 700 times.

### Gray-level slicing

Highlighting a specific range of gray levels in an image often is desired. Applications include enhancing features such as masses of water in satellite imagery and enhancing flaws in X-ray images. There are several ways of doing level slicing, but most of them are variations of two basic themes. One approach is to display a high value for all gray levels in the range of interest and a low value for all other gray levels. This transformation, shown in Fig. 3.11(a), produces a binary image. The second approach, based on the transformation shown in Fig. 3.11(b), brightens the desired range of gray levels but preserves the background and gray-level tonalities in the image. Figure 3.11(c) shows a gray-scale image, and Fig. 3.11(d) shows the result of using the transformation in Fig. 3.11(a). Variations of the two transformations shown in Fig. 3.11 are easy to formulate.

### Bit-plane slicing

Instead of highlighting gray-level ranges, highlighting the contribution made to total image appearance by specific bits might be desired. Suppose that each pixel in an image is represented by 8 bits. Imagine that the image is composed of eight 1-bit planes, ranging from bit-plane 0 for the least significant bit to bit-plane 7 for the most significant bit. In terms of 8-bit bytes, plane 0 contains all the lowest order bits in the bytes comprising the pixels in the image and plane 7 contains all the high-order bits. Figure 3.12 illustrates these ideas, and Fig. 3.14 shows the various bit planes for the image shown in Fig. 3.13. Note that the higher-order bits (especially the top four) contain the majority of the visually significant data. The other bit planes contribute to more subtle details in the image. Separating a digital image into its bit planes is useful for analyzing the relative importance played by each bit of the image, a process that aids in determining the adequacy of the number of bits used to quantize each pixel. Also, this type of decomposition is useful for image compression, as discussed in Chapter 8.



**a b**  
**c d**

**FIGURE 3.11**  
(a) This transformation highlights range  $[A, B]$  of gray levels and reduces all others to a constant level. (b) This transformation highlights range  $[A, B]$  but preserves all other levels. (c) An image. (d) Result of using the transformation in (a).

In terms of bit-plane extraction for an 8-bit image, it is not difficult to show that the (binary) image for bit-plane 7 can be obtained by processing the input image with a thresholding gray-level transformation function that (1) maps all levels in the image between 0 and 127 to one level (for example, 0); and (2) maps all levels between 129 and 255 to another (for example, 255). The binary image for bit-plane 7 in Fig. 3.14 was obtained in just this manner. It is left as an exercise (Problem 3.3) to obtain the gray-level transformation functions that would yield the other bit planes.

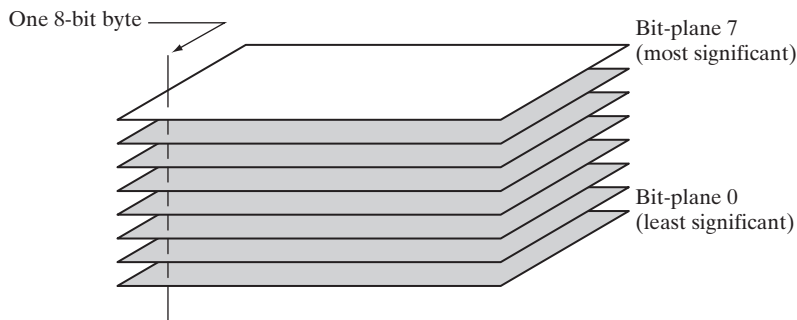


**FIGURE 3.12**  
Bit-plane representation of an 8-bit image.

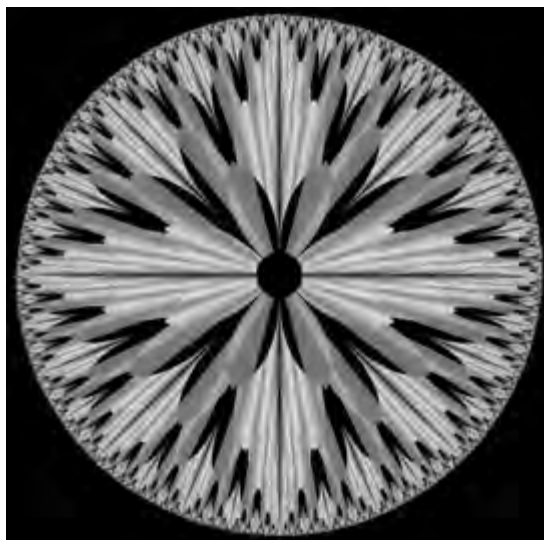


**FIGURE 3.13** An 8-bit fractal image. (A fractal is an image generated from mathematical expressions). (Courtesy of Ms. Melissa D. Binde, Swarthmore College, Swarthmore, PA.)



See inside front cover  
Consult the book web site  
for a review of basic probability theory.

### 3.3 Histogram Processing

The histogram of a digital image with gray levels in the range  $[0, L - 1]$  is a discrete function  $h(r_k) = n_k$ , where  $r_k$  is the  $k$ th gray level and  $n_k$  is the number of pixels in the image having gray level  $r_k$ . It is common practice to normalize a histogram by dividing each of its values by the total number of pixels in the image, denoted by  $n$ . Thus, a normalized histogram is given by  $p(r_k) = n_k/n$ , for  $k = 0, 1, \dots, L - 1$ . Loosely speaking,  $p(r_k)$  gives an estimate of the probability of occurrence of gray level  $r_k$ . Note that the sum of all components of a normalized histogram is equal to 1.

Histograms are the basis for numerous spatial domain processing techniques. Histogram manipulation can be used effectively for image enhancement, as shown in this section. In addition to providing useful image statistics, we shall see in subsequent chapters that the information inherent in histograms also is quite useful in other image processing applications, such as image compression and segmentation. Histograms are simple to calculate in software and also lend themselves to economic hardware implementations, thus making them a popular tool for real-time image processing.

As an introduction to the role of histogram processing in image enhancement, consider Fig. 3.15, which is the pollen image of Fig. 3.10 shown in four basic gray-level characteristics: dark, light, low contrast, and high contrast. The right side of the figure shows the histograms corresponding to these images. The horizontal axis of each histogram plot corresponds to gray level values,  $r_k$ . The vertical axis corresponds to values of  $h(r_k) = n_k$  or  $p(r_k) = n_k/n$  if the values are normalized. Thus, as indicated previously, these histogram plots are simply plots of  $h(r_k) = n_k$  versus  $r_k$  or  $p(r_k) = n_k/n$  versus  $r_k$ .

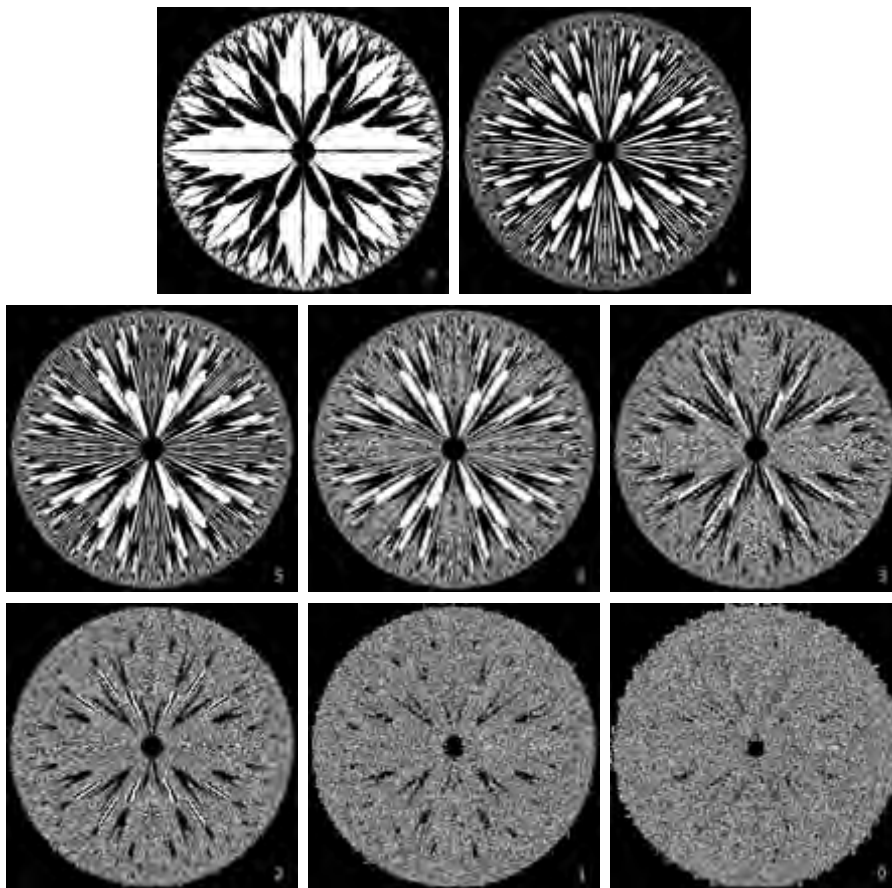
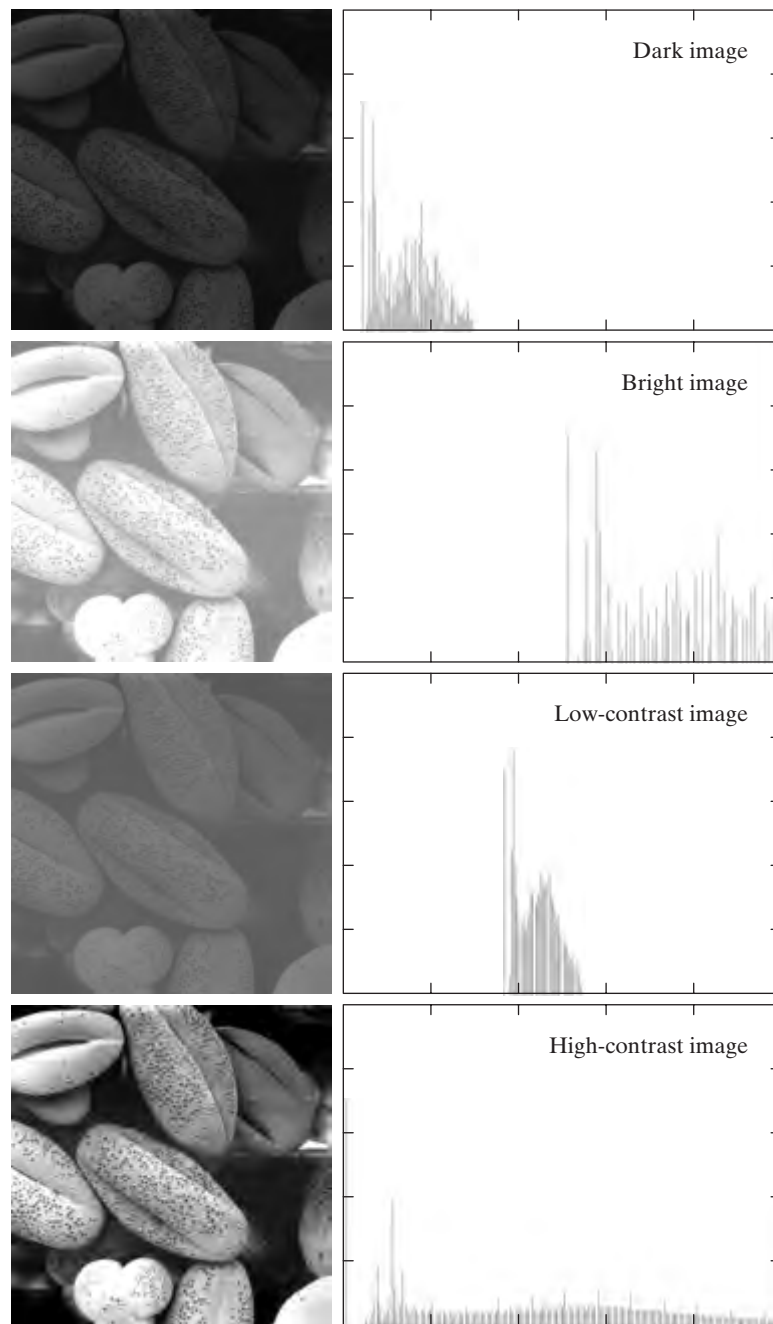


**FIGURE 3.14** The eight bit planes of the image in Fig. 3.13. The number at the bottom, right of each image identifies the bit plane.

We note in the dark image that the components of the histogram are concentrated on the low (dark) side of the gray scale. Similarly, the components of the histogram of the bright image are biased toward the high side of the gray scale. An image with low contrast has a histogram that will be narrow and will be centered toward the middle of the gray scale. For a monochrome image this implies a dull, washed-out gray look. Finally, we see that the components of the histogram in the high-contrast image cover a broad range of the gray scale and, further, that the distribution of pixels is not too far from uniform, with very few vertical lines being much higher than the others. Intuitively, it is reasonable to conclude that an image whose pixels tend to occupy the entire range of possible gray levels and, in addition, tend to be distributed uniformly, will have an appearance of high contrast and will exhibit a large variety of gray tones. The net effect will be an image that shows a great deal of gray-level detail and has high dynamic range. It will be shown shortly that it is possible to develop a transformation function that can automatically achieve this effect, based only on information available in the histogram of the input image.



a b

**FIGURE 3.15** Four basic image types: dark, light, low contrast, high contrast, and their corresponding histograms. (Original image courtesy of Dr. Roger Heady, Research School of Biological Sciences, Australian National University, Canberra, Australia.)



### 3.3.1 Histogram Equalization

Consider for a moment continuous functions, and let the variable  $r$  represent the gray levels of the image to be enhanced. In the initial part of our discussion we assume that  $r$  has been normalized to the interval  $[0, 1]$ , with  $r = 0$  representing black and  $r = 1$  representing white. Later, we consider a discrete formulation and allow pixel values to be in the interval  $[0, L - 1]$ .

For any  $r$  satisfying the aforementioned conditions, we focus attention on transformations of the form

$$s = T(r) \quad 0 \leq r \leq 1 \quad (3.3-1)$$

that produce a level  $s$  for every pixel value  $r$  in the original image. For reasons that will become obvious shortly, we assume that the transformation function  $T(r)$  satisfies the following conditions:

- (a)  $T(r)$  is single-valued and monotonically increasing in the interval  $0 \leq r \leq 1$ ; and
- (b)  $0 \leq T(r) \leq 1$  for  $0 \leq r \leq 1$ .

The requirement in (a) that  $T(r)$  be single valued is needed to guarantee that the inverse transformation will exist, and the monotonicity condition preserves the increasing order from black to white in the output image. A transformation function that is not monotonically increasing could result in at least a section of the intensity range being inverted, thus producing some inverted gray levels in the output image. While this may be a desirable effect in some cases, that is not what we are after in the present discussion. Finally, condition (b) guarantees that the output gray levels will be in the same range as the input levels. Figure 3.16 gives an example of a transformation function that satisfies these two conditions. The inverse transformation from  $s$  back to  $r$  is denoted

$$r = T^{-1}(s) \quad 0 \leq s \leq 1. \quad (3.3-2)$$

It can be shown by example (Problem 3.8) that even if  $T(r)$  satisfies conditions (a) and (b), it is possible that the corresponding inverse  $T^{-1}(s)$  may fail to be single valued.

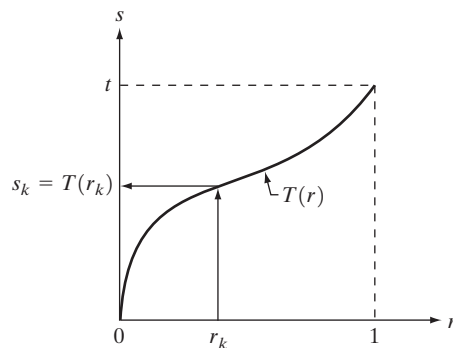


**FIGURE 3.16** A gray-level transformation function that is both single valued and monotonically increasing.

The gray levels in an image may be viewed as random variables in the interval  $[0, 1]$ . One of the most fundamental descriptors of a random variable is its probability density function (PDF). Let  $p_r(r)$  and  $p_s(s)$  denote the probability density functions of random variables  $r$  and  $s$ , respectively, where the subscripts on  $p$  are used to denote that  $p_r$  and  $p_s$  are different functions. A basic result from an elementary probability theory is that, if  $p_r(r)$  and  $T(r)$  are known and  $T^{-1}(s)$  satisfies condition (a), then the probability density function  $p_s(s)$  of the transformed variable  $s$  can be obtained using a rather simple formula:

$$p_s(s) = p_r(r) \left| \frac{dr}{ds} \right|. \quad (3.3-3)$$

Thus, the probability density function of the transformed variable,  $s$ , is determined by the gray-level PDF of the input image and by the chosen transformation function.

A transformation function of particular importance in image processing has the form

$$s = T(r) = \int_0^r p_r(w) dw \quad (3.3-4)$$

where  $w$  is a dummy variable of integration. The right side of Eq. (3.3-4) is recognized as the cumulative distribution function (CDF) of random variable  $r$ . Since probability density functions are always positive, and recalling that the integral of a function is the area under the function, it follows that this transformation function is single valued and monotonically increasing, and, therefore, satisfies condition (a). Similarly, the integral of a probability density function for variables in the range  $[0, 1]$  also is in the range  $[0, 1]$ , so condition (b) is satisfied as well.

Given transformation function  $T(r)$ , we find  $p_s(s)$  by applying Eq. (3.3-3). We know from basic calculus (Leibniz's rule) that the derivative of a definite integral with respect to its upper limit is simply the integrand evaluated at that limit. In other words,

$$\begin{aligned} \frac{ds}{dr} &= \frac{dT(r)}{dr} \\ &= \frac{d}{dr} \left[ \int_0^r p_r(w) dw \right] \\ &= p_r(r). \end{aligned} \quad (3.3-5)$$

Substituting this result for  $dr/ds$  into Eq. (3.3-3), and keeping in mind that all probability values are positive, yields

$$\begin{aligned} p_s(s) &= p_r(r) \left| \frac{dr}{ds} \right| \\ &= p_r(r) \left| \frac{1}{p_r(r)} \right| \\ &= 1 \quad 0 \leq s \leq 1. \end{aligned} \quad (3.3-6)$$

Because  $p_s(s)$  is a probability density function, it follows that it must be zero outside the interval  $[0, 1]$  in this case because its integral over all values of  $s$  must equal 1. We recognize the form of  $p_s(s)$  given in Eq. (3.3-6) as a *uniform* probability density function. Simply stated, we have demonstrated that performing the transformation function given in Eq. (3.3-4) yields a random variable  $s$  characterized by a uniform probability density function. It is important to note from Eq. (3.3-4) that  $T(r)$  depends on  $p_r(r)$ , but, as indicated by Eq. (3.3-6), the resulting  $p_s(s)$  *always* is uniform, *independent* of the form of  $p_r(r)$ .

For discrete values we deal with probabilities and summations instead of probability density functions and integrals. The probability of occurrence of gray level  $r_k$  in an image is approximated by

$$p_r(r_k) = \frac{n_k}{n} \quad k = 0, 1, 2, \dots, L - 1 \quad (3.3-7)$$

where, as noted at the beginning of this section,  $n$  is the total number of pixels in the image,  $n_k$  is the number of pixels that have gray level  $r_k$ , and  $L$  is the total number of possible gray levels in the image. The discrete version of the transformation function given in Eq. (3.3-4) is

$$\begin{aligned} s_k = T(r_k) &= \sum_{j=0}^k p_r(r_j) \\ &= \sum_{j=0}^k \frac{n_j}{n} \quad k = 0, 1, 2, \dots, L - 1. \end{aligned} \quad (3.3-8)$$

Thus, a processed (output) image is obtained by mapping each pixel with level  $r_k$  in the input image into a corresponding pixel with level  $s_k$  in the output image via Eq. (3.3-8). As indicated earlier, a plot of  $p_r(r_k)$  versus  $r_k$  is called a *histogram*. The transformation (mapping) given in Eq. (3.3-8) is called *histogram equalization* or *histogram linearization*. It is not difficult to show (Problem 3.9) that the transformation in Eq. (3.3-8) satisfies conditions (a) and (b) stated previously in this section.

Unlike its continuous counterpart, it cannot be proved in general that this discrete transformation will produce the discrete equivalent of a uniform probability density function, which would be a uniform histogram. However, as will be seen shortly, use of Eq. (3.3-8) does have the general tendency of spreading the histogram of the input image so that the levels of the histogram-equalized image will span a fuller range of the gray scale.

We discussed earlier in this section the many advantages of having gray-level values that cover the entire gray scale. In addition to producing gray levels that have this tendency, the method just derived has the additional advantage that it is fully “automatic.” In other words, given an image, the process of histogram equalization consists simply of implementing Eq. (3.3-8), which is based on information that can be extracted directly from the given image, without the need for further parameter specifications. We note also the simplicity of the computations that would be required to implement the technique.

The inverse transformation from  $s$  back to  $r$  is denoted by

$$r_k = T^{-1}(s_k) \quad k = 0, 1, 2, \dots, L - 1 \quad (3.3-9)$$

It can be shown (Problem 3.9) that the inverse transformation in Eq. (3.3-9) satisfies conditions (a) and (b) stated previously in this section only if none of the levels,  $r_k, k = 0, 1, 2, \dots, L - 1$ , are missing from the input image. Although the inverse transformation is not used in histogram equalization, it plays a central role in the histogram-matching scheme developed in the next section. We also discuss in that section details of how to implement histogram processing techniques.

**EXAMPLE 3.3:**  
Histogram  
equalization.

■ Figure 3.17(a) shows the four images from Fig. 3.15, and Fig. 3.17(b) shows the result of performing histogram equalization on each of these images. The first three results (top to bottom) show significant improvement. As expected, histogram equalization did not produce a significant visual difference in the fourth image because the histogram of this image already spans the full spectrum of the gray scale. The transformation functions used to generate the images in Fig. 3.17(b) are shown in Fig. 3.18. These functions were generated from the histograms of the original images [see Fig. 3.15(b)] using Eq. (3.3-8). Note that transformation (4) has a basic linear shape, again indicating that the gray levels in the fourth input image are nearly uniformly distributed. As was just noted, we would expect histogram equalization in this case to have negligible effect on the appearance of the image.

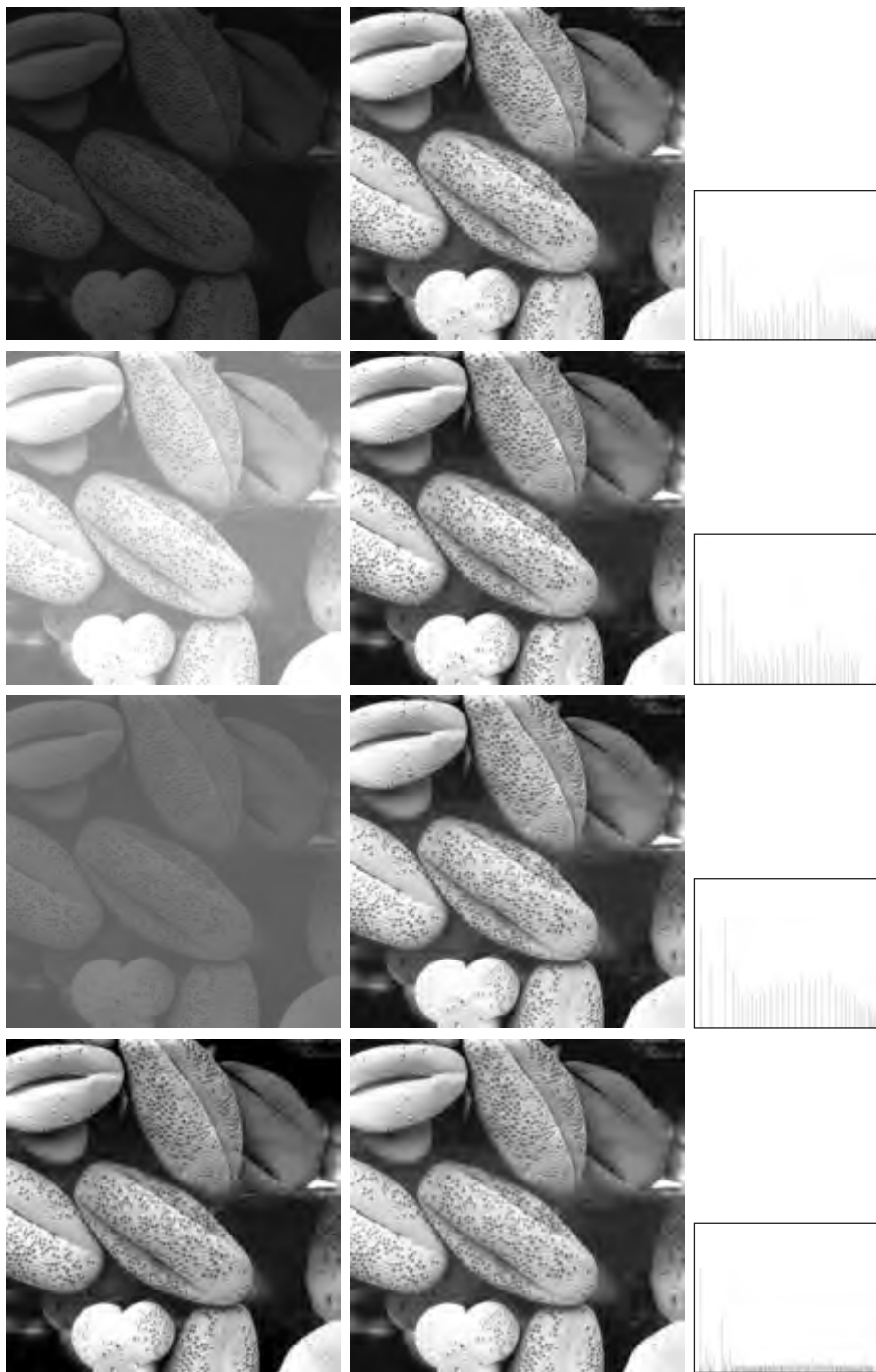
The histograms of the equalized images are shown in Fig. 3.17(c). It is of interest to note that, while all these histograms are different, the histogram-equalized images themselves are visually very similar. This is not unexpected because the difference between the images in the left column is simply one of contrast, not of content. In other words, since the images have the same content, the increase in contrast resulting from histogram equalization was enough to render any gray-level differences in the resulting images visually indistinguishable. Given the significant contrast differences of the images in the left column, this example illustrates the power of histogram equalization as an adaptive enhancement tool. ■

### 3.3.2 Histogram Matching (Specification)

As indicated in the preceding discussion, histogram equalization automatically determines a transformation function that seeks to produce an output image that has a uniform histogram. When automatic enhancement is desired, this is a good approach because the results from this technique are predictable and the method is simple to implement. We show in this section that there are applications in which attempting to base enhancement on a uniform histogram is not the best approach. In particular, it is useful sometimes to be able to specify the shape of the histogram that we wish the processed image to have. The method used to generate a processed image that has a specified histogram is called *histogram matching* or *histogram specification*.

#### Development of the method

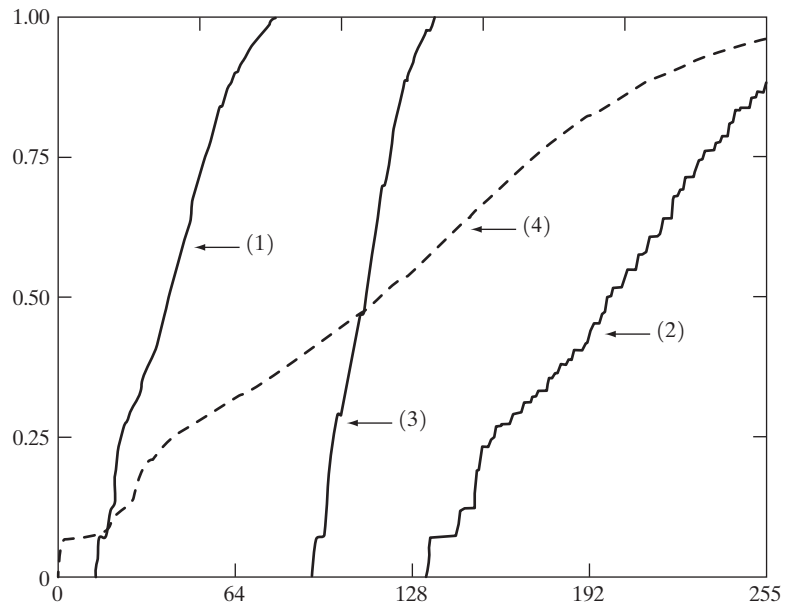
Let us return for a moment to continuous gray levels  $r$  and  $z$  (considered continuous random variables), and let  $p_r(r)$  and  $p_z(z)$  denote their corresponding continuous probability density functions. In this notation,  $r$  and  $z$  denote



a b c

**FIGURE 3.17** (a) Images from Fig. 3.15. (b) Results of histogram equalization. (c) Corresponding histograms.

**FIGURE 3.18**  
Transformation functions (1) through (4) were obtained from the histograms of the images in Fig.3.17(a), using Eq. (3.3-8).



the gray levels of the input and output (processed) images, respectively. We can estimate  $p_r(r)$  from the given input image, while  $p_z(z)$  is the *specified* probability density function that we wish the output image to have.

Let  $s$  be a random variable with the property

$$s = T(r) = \int_0^r p_r(w) dw \quad (3.3-10)$$

where  $w$  is a dummy variable of integration. We recognize this expression as the continuous version of histogram equalization given in Eq. (3.3-4). Suppose next that we define a random variable  $z$  with the property

$$G(z) = \int_0^z p_z(t) dt = s \quad (3.3-11)$$

where  $t$  is a dummy variable of integration. It then follows from these two equations that  $G(z) = T(r)$  and, therefore, that  $z$  must satisfy the condition

$$z = G^{-1}(s) = G^{-1}[T(r)]. \quad (3.3-12)$$

The transformation  $T(r)$  can be obtained from Eq. (3.3-10) once  $p_r(r)$  has been estimated from the input image. Similarly, the transformation function  $G(z)$  can be obtained using Eq. (3.3-11) because  $p_z(z)$  is given.

Assuming that  $G^{-1}$  exists and that it satisfies conditions (a) and (b) in the previous section, Eqs. (3.3-10) through (3.3-12) show that an image with a specified probability density function can be obtained from an input image by using the following procedure: (1) Obtain the transformation function  $T(r)$  using Eq. (3.3-10). (2) Use Eq. (3.3-11) to obtain the transformation function  $G(z)$ . (3) Obtain the inverse transformation function  $G^{-1}$ . (4) Obtain the output image

by applying Eq. (3.3-12) to all the pixels in the input image. The result of this procedure will be an image whose gray levels,  $z$ , have the specified probability density function  $p_z(z)$ .

Although the procedure just described is straightforward in principle, it is seldom possible in practice to obtain analytical expressions for  $T(r)$  and for  $G^{-1}$ . Fortunately, this problem is simplified considerably in the case of discrete values. The price we pay is the same as in histogram equalization, where only an approximation to the desired histogram is achievable. In spite of this, however, some very useful results can be obtained even with crude approximations.

The discrete formulation of Eq. (3.3-10) is given by Eq. (3.3-8), which we repeat here for convenience:

$$\begin{aligned} s_k &= T(r_k) = \sum_{j=0}^k p_r(r_j) \\ &= \sum_{j=0}^k \frac{n_j}{n} \quad k = 0, 1, 2, \dots, L - 1 \end{aligned} \quad (3.3-13)$$

where  $n$  is the total number of pixels in the image,  $n_j$  is the number of pixels with gray level  $r_j$ , and  $L$  is the number of discrete gray levels. Similarly, the discrete formulation of Eq. (3.3-11) is obtained from the given histogram  $p_z(z_i)$ ,  $i = 0, 1, 2, \dots, L - 1$ , and has the form

$$v_k = G(z_k) = \sum_{i=0}^k p_z(z_i) = s_k \quad k = 0, 1, 2, \dots, L - 1. \quad (3.3-14)$$

As in the continuous case, we are seeking values of  $z$  that satisfy this equation. The variable  $v_k$  was added here for clarity in the discussion that follows. Finally, the discrete version of Eq. (3.3-12) is given by

$$z_k = G^{-1}[T(r_k)] \quad k = 0, 1, 2, \dots, L - 1 \quad (3.3-15)$$

or, from Eq. (3.3-13),

$$z_k = G^{-1}(s_k) \quad k = 0, 1, 2, \dots, L - 1. \quad (3.3-16)$$

Equations (3.3-13) through (3.3-16) are the foundation for implementing histogram matching for digital images. Equation (3.3-13) is a mapping from the levels in the original image into corresponding levels  $s_k$  based on the histogram of the original image, which we compute from the pixels in the image. Equation (3.3-14) computes a transformation function  $G$  from the given histogram  $p_z(z)$ . Finally, Eq. (3.3-15) or its equivalent, Eq. (3.3-16), gives us (an approximation of) the desired levels of the image with that histogram. The first two equations can be implemented easily because all the quantities are known. Implementation of Eq. (3.3-16) is straightforward, but requires additional explanation.

### Implementation

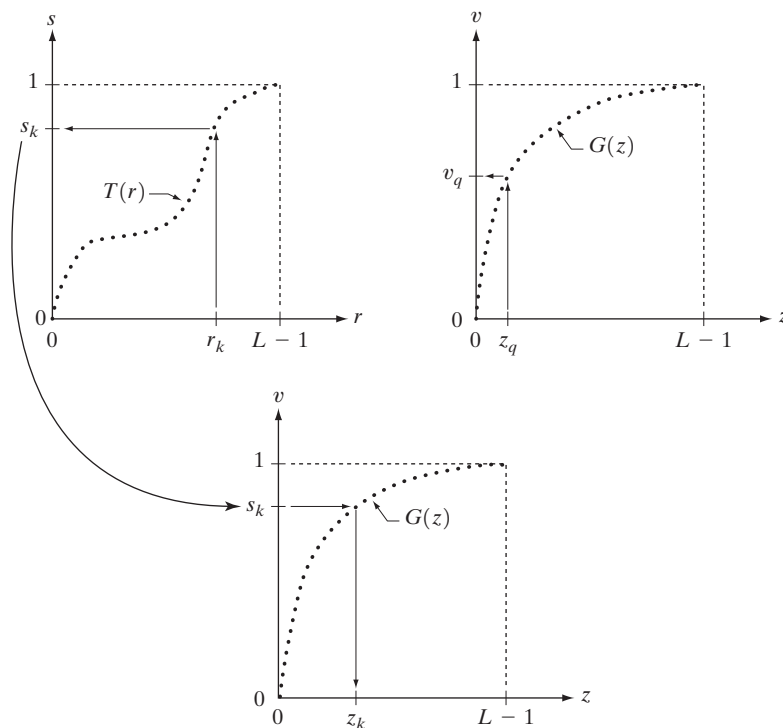
We start by noting the following: (1) Each set of gray levels  $\{r_j\}$ ,  $\{s_j\}$ , and  $\{z_j\}$ ,  $j = 0, 1, 2, \dots, L - 1$ , is a one-dimensional array of dimension  $L \times 1$ . (2) All mappings from  $r$  to  $s$  and from  $s$  to  $z$  are simple table lookups between a given

pixel value and these arrays. (3) Each of the elements of these arrays, for example,  $s_k$ , contains two important pieces of information: The subscript  $k$  denotes the location of the element in the array, and  $s$  denotes the value at that location. (4) We need to be concerned only with integer pixel values. For example, in the case of an 8-bit image,  $L = 256$  and the elements of each of the arrays just mentioned are integers between 0 and 255. This implies that we now work with gray level values in the interval  $[0, L - 1]$  instead of the normalized interval  $[0, 1]$  that we used before to simplify the development of histogram processing techniques.

In order to see how histogram matching actually can be implemented, consider Fig. 3.19(a), ignoring for a moment the connection shown between this figure and Fig. 3.19(c). Figure 3.19(a) shows a hypothetical discrete transformation function  $s = T(r)$  obtained from a given image. The first gray level in the image,  $r_1$ , maps to  $s_1$ ; the second gray level,  $r_2$ , maps to  $s_2$ ; the  $k$ th level  $r_k$  maps to  $s_k$ ; and so on (the important point here is the *ordered* correspondence between these values). Each value  $s_j$  in the array is precomputed using Eq. (3.3-13), so the process of mapping simply uses the actual value of a pixel as an index in an array to determine the corresponding value of  $s$ . This process is particularly easy because we are dealing with integers. For example, the  $s$  mapping for an 8-bit pixel with value 127 would be found in the 128th position in array  $\{s_j\}$  (recall that we start at 0) out of the possible 256 positions. If we stopped here and mapped the value of each pixel of an input image by the

a b  
c

**FIGURE 3.19**  
(a) Graphical interpretation of mapping from  $r_k$  to  $s_k$  via  $T(r)$ .  
(b) Mapping of  $z_q$  to its corresponding value  $v_q$  via  $G(z)$ .  
(c) Inverse mapping from  $s_k$  to its corresponding value of  $z_k$ .





method just described, the output would be a histogram-equalized image, according to Eq. (3.3-8).

In order to implement histogram matching we have to go one step further. Figure 3.19(b) is a hypothetical transformation function  $G$  obtained from a given histogram  $p_z(z)$  by using Eq. (3.3-14). For any  $z_q$ , this transformation function yields a corresponding value  $v_q$ . This mapping is shown by the arrows in Fig. 3.19(b). Conversely, given any value  $v_q$ , we would find the corresponding value  $z_q$  from  $G^{-1}$ . In terms of the figure, all this means graphically is that we would reverse the direction of the arrows to map  $v_q$  into its corresponding  $z_q$ . However, we know from the definition in Eq. (3.3-14) that  $v = s$  for corresponding subscripts, so we can use exactly this process to find the  $z_k$  corresponding to any value  $s_k$  that we computed previously from the equation  $s_k = T(r_k)$ . This idea is shown in Fig. 3.19(c).

Since we really do not have the  $z$ 's (recall that finding these values is precisely the objective of histogram matching), we must resort to some sort of iterative scheme to find  $z$  from  $s$ . The fact that we are dealing with integers makes this a particularly simple process. Basically, because  $v_k = s_k$ , we have from Eq. (3.3-14) that the  $z$ 's for which we are looking must satisfy the equation  $G(z_k) = s_k$ , or  $(G(z_k) - s_k) = 0$ . Thus, all we have to do to find the value of  $z_k$  corresponding to  $s_k$  is to iterate on values of  $z$  such that this equation is satisfied for  $k = 0, 1, 2, \dots, L - 1$ . This is the same thing as Eq. (3.3-16), except that we do not have to find the inverse of  $G$  because we are going to iterate on  $z$ . Since we are dealing with integers, the closest we can get to satisfying the equation  $(G(z_k) - s_k) = 0$  is to let  $z_k = \hat{z}$  for each value of  $k$ , where  $\hat{z}$  is the *smallest* integer in the interval  $[0, L - 1]$  such that

$$(G(\hat{z}) - s_k) \geq 0 \quad k = 0, 1, 2, \dots, L - 1. \quad (3.3-17)$$

Given a value  $s_k$ , all this means conceptually in terms of Fig. 3.19(c) is that we would start with  $\hat{z} = 0$  and increase it in integer steps until Eq. (3.3-17) is satisfied, at which point we let  $z_k = \hat{z}$ . Repeating this process for all values of  $k$  would yield all the required mappings from  $s$  to  $z$ , which constitutes the implementation of Eq. (3.3-16). In practice, we would not have to start with  $\hat{z} = 0$  each time because the values of  $s_k$  are known to increase monotonically. Thus, for  $k = k + 1$ , we would start with  $\hat{z} = z_k$  and increment in integer values from there.

The procedure we have just developed for histogram matching may be summarized as follows:

1. Obtain the histogram of the given image.
2. Use Eq. (3.3-13) to precompute a mapped level  $s_k$  for each level  $r_k$ .
3. Obtain the transformation function  $G$  from the given  $p_z(z)$  using Eq. (3.3-14).
4. Precompute  $z_k$  for each value of  $s_k$  using the iterative scheme defined in connection with Eq. (3.3-17).
5. For each pixel in the original image, if the value of that pixel is  $r_k$ , map this value to its corresponding level  $s_k$ ; then map level  $s_k$  into the final level  $z_k$ . Use the precomputed values from Steps (2) and (4) for these mappings.

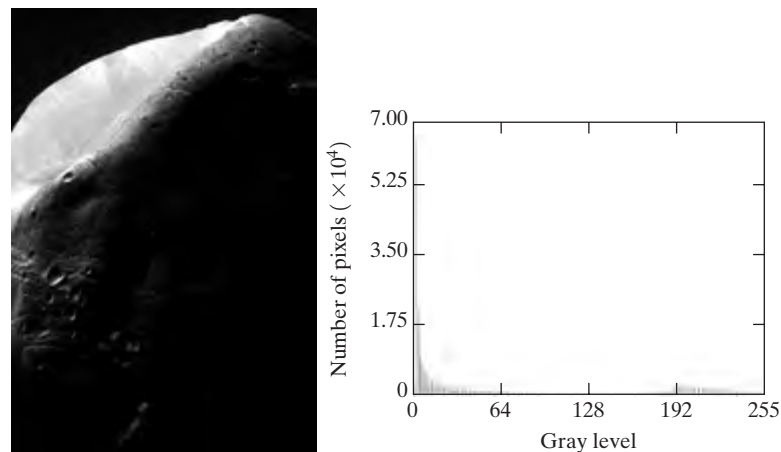
Note that Step (5) implements two mappings for each pixel in the image being processed. The first mapping is nothing more than histogram equalization. If the histogram-equalized image is not required, it obviously would be beneficial to combine both transformations into one in order to save an intermediate step.

Finally, we note that, even in the discrete case, we need to be concerned about  $G^{-1}$  satisfying conditions (a) and (b) of the previous section. It is not difficult to show (Problem 3.9) that the only way to guarantee that  $G^{-1}$  be single valued and monotonic is to require that  $G$  be strictly monotonic (i.e., always increasing), which means simply that none of the values of the specified histogram  $p_z(z_i)$  in Eq. (3.3-14) can be zero.

**EXAMPLE 3.4:** Comparison between histogram equalization and histogram matching.

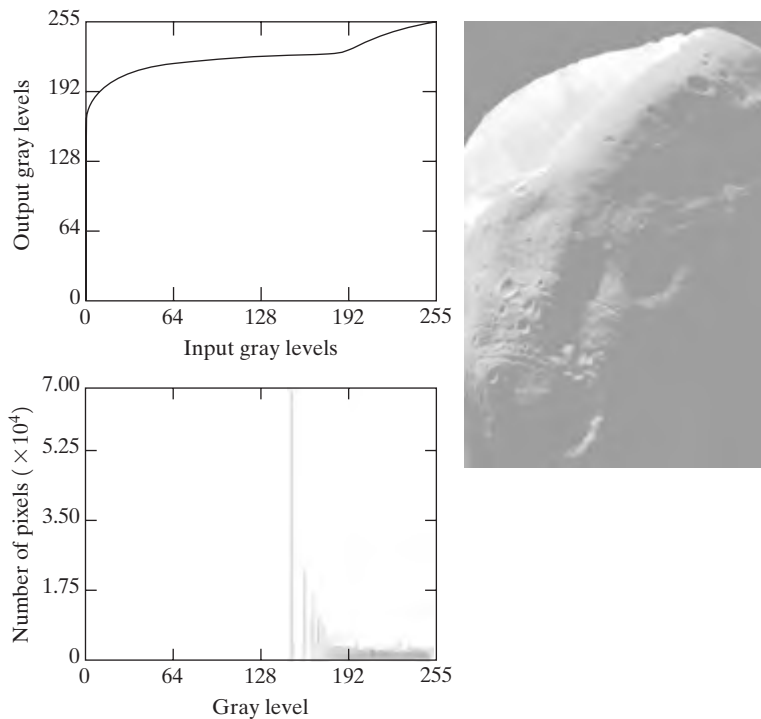
■ Figure 3.20(a) shows an image of the Mars moon, Phobos, taken by NASA's *Mars Global Surveyor*. Figure 3.20(b) shows the histogram of Fig. 3.20(a). The image is dominated by large, dark areas, resulting in a histogram characterized by a large concentration of pixels in the dark end of the gray scale. At first glance, one might conclude that histogram equalization would be a good approach to enhance this image, so that details in the dark areas become more visible. It is demonstrated in the following discussion that this is not so.

Figure 3.21(a) shows the histogram equalization transformation [Eq. (3.3-8) or (3.3-13)] obtained from the histogram shown in Fig. 3.20(b). The most relevant characteristic of this transformation function is how fast it rises from gray level 0 to a level near 190. This is caused by the large concentration of pixels in the input histogram having levels very near 0. When this transformation is applied to the levels of the input image to obtain a histogram-equalized result, the net effect is to map a very narrow interval of dark pixels into the upper end of the gray scale of the output image. Because numerous pixels in the input image have levels precisely in this interval, we would expect the result to be an



a b

**FIGURE 3.20** (a) Image of the Mars moon Photos taken by NASA's *Mars Global Surveyor*. (b) Histogram. (Original image courtesy of NASA.)



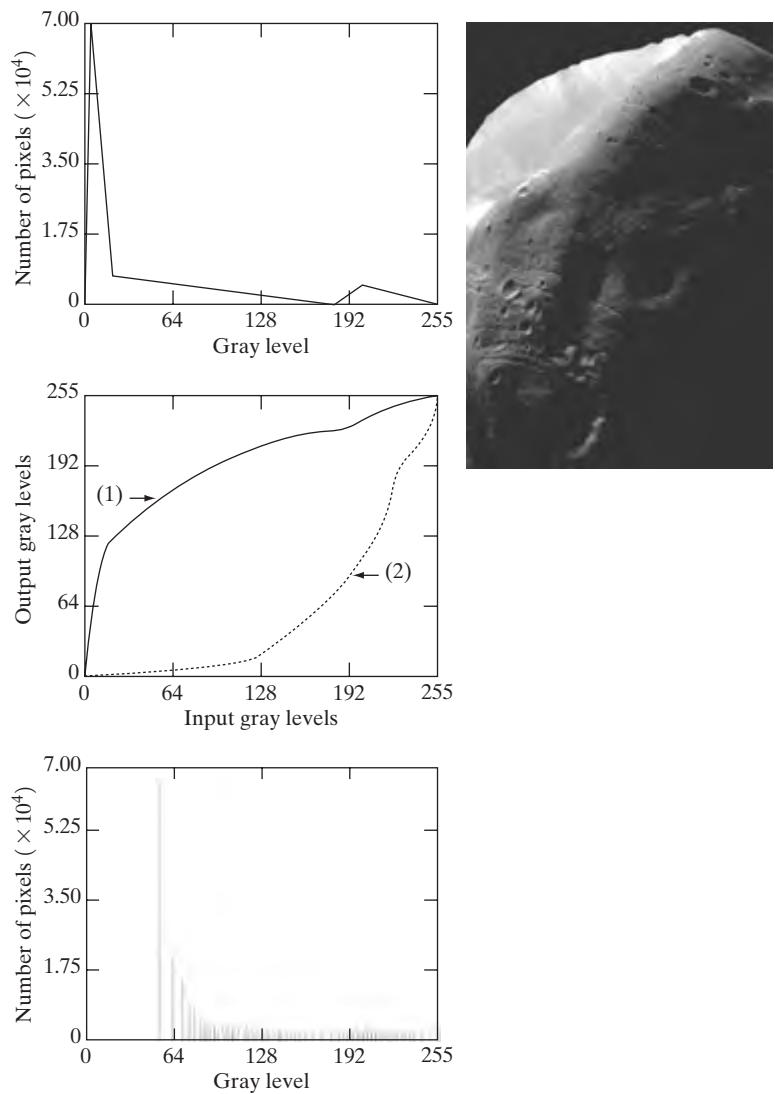
**FIGURE 3.21**  
 (a) Transformation function for histogram equalization.  
 (b) Histogram-equalized image (note the washed-out appearance).  
 (c) Histogram of (b).

image with a light, washed-out appearance. As shown in Fig. 3.21(b), this is indeed the case. The histogram of this image is shown in Fig. 3.21(c). Note how all the gray levels are biased toward the upper one-half of the gray scale.

Since the problem with the transformation function in Fig. 3.21(a) was caused by a large concentration of pixels in the original image with levels near 0, a reasonable approach is to modify the histogram of that image so that it does not have this property. Figure 3.22(a) shows a *manually specified* function that preserves the general shape of the original histogram, but has a smoother transition of levels in the dark region of the gray scale. Sampling this function into 256 equally spaced discrete values produced the desired specified histogram. The transformation function  $G(z)$  obtained from this histogram using Eq. (3.3-14) is labeled transformation (1) in Fig. 3.22(b). Similarly, the inverse transformation  $G^{-1}(s)$  from Eq. (3.3-16) [obtained using the iterative technique discussed in connection with Eq. (3.3-17)] is labeled transformation (2) in Fig. 3.22(b). The enhanced image in Fig. 3.22(c) was obtained by applying transformation (2) to the pixels of the histogram-equalized image in Fig. 3.21(b). The improvement of the histogram-specified image over the result obtained by histogram equalization is evident by comparing these two images. It is of interest to note that a rather modest change in the original histogram was all that was required to obtain a significant improvement in enhancement. The histogram of Fig. 3.22(c) is shown in Fig. 3.22(d). The most distinguishing feature of this histogram is how its low end has shifted right toward the lighter region of the gray scale, as desired. ■

a c  
b  
d

**FIGURE 3.22**  
 (a) Specified histogram.  
 (b) Curve (1) is from Eq. (3.3-14), using the histogram in (a); curve (2) was obtained using the iterative procedure in Eq. (3.3-17).  
 (c) Enhanced image using mappings from curve (2).  
 (d) Histogram of (c).



Although it probably is obvious by now, we emphasize before leaving this section that histogram specification is, for the most part, a trial-and-error process. One can use guidelines learned from the problem at hand, just as we did in the preceding example. At times, there may be cases in which it is possible to formulate what an “average” histogram should look like and use that as the specified histogram. In cases such as these, histogram specification becomes a straightforward process. In general, however, there are no rules for specifying histograms, and one must resort to analysis on a case-by-case basis for any given enhancement task.

### 3.3.3 Local Enhancement

The histogram processing methods discussed in the previous two sections are *global*, in the sense that pixels are modified by a transformation function based on the gray-level content of an entire image. Although this global approach is suitable for overall enhancement, there are cases in which it is necessary to enhance details over small areas in an image. The number of pixels in these areas may have negligible influence on the computation of a global transformation whose shape does not necessarily guarantee the desired local enhancement. The solution is to devise transformation functions based on the gray-level distribution—or other properties—in the neighborhood of every pixel in the image. Although processing methods based on neighborhoods are the topic of Section 3.5, we discuss local histogram processing here for the sake of clarity and continuity. The reader will have no difficulty in following the discussion.

The histogram processing techniques previously described are easily adaptable to local enhancement. The procedure is to define a square or rectangular neighborhood and move the center of this area from pixel to pixel. At each location, the histogram of the points in the neighborhood is computed and either a histogram equalization or histogram specification transformation function is obtained. This function is finally used to map the gray level of the pixel centered in the neighborhood. The center of the neighborhood region is then moved to an adjacent pixel location and the procedure is repeated. Since only one new row or column of the neighborhood changes during a pixel-to-pixel translation of the region, updating the histogram obtained in the previous location with the new data introduced at each motion step is possible (Problem 3.11). This approach has obvious advantages over repeatedly computing the histogram over all pixels in the neighborhood region each time the region is moved one pixel location. Another approach used some times to reduce computation is to utilize nonoverlapping regions, but this method usually produces an undesirable checkerboard effect.

■ Figure 3.23(a) shows an image that has been slightly blurred to reduce its noise content (see Section 3.6.1 regarding blurring). Figure 3.23(b) shows the result of global histogram equalization. As is often the case when this technique is applied to smooth, noisy areas, Fig. 3.23(b) shows considerable enhancement of the noise, with a slight increase in contrast. Note that no new structural details were brought out by this method. However, local histogram equalization using a  $7 \times 7$  neighborhood revealed the presence of small squares inside the larger dark squares. The small squares were too close in gray level to the larger ones, and their sizes were too small to influence global histogram equalization significantly. Note also the finer noise texture in Fig. 3.23(c), a result of local processing using relatively small neighborhoods. ■

**EXAMPLE 3.5:**  
Enhancement  
using local  
histograms.

### 3.3.4 Use of Histogram Statistics for Image Enhancement

Instead of using the image histogram directly for enhancement, we can use instead some statistical parameters obtainable directly from the histogram. Let  $r$  denote a discrete random variable representing discrete gray-levels in the range

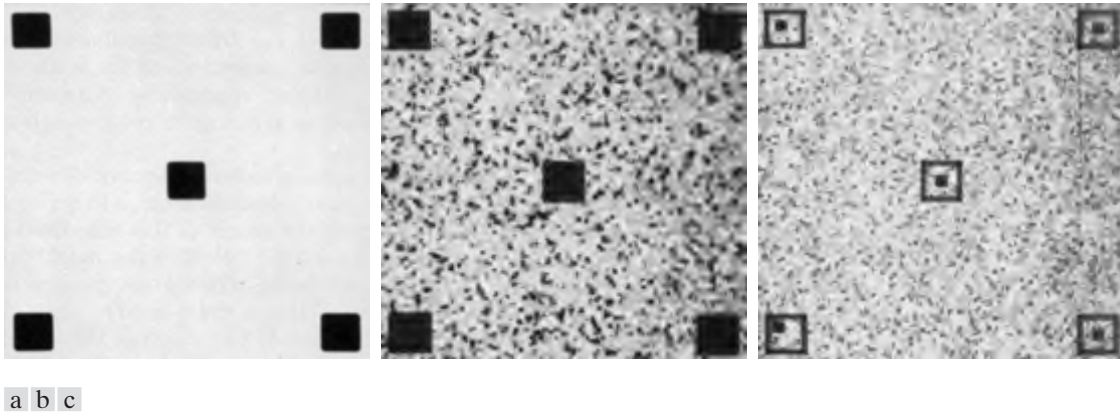


**FIGURE 3.23** (a) Original image. (b) Result of global histogram equalization. (c) Result of local histogram equalization using a  $7 \times 7$  neighborhood about each pixel.

$[0, L - 1]$ , and let  $p(r_i)$  denote the normalized histogram component corresponding to the  $i$ th value of  $r$ . As indicated previously in this section, we may view  $p(r_i)$  as an estimate of the probability of occurrence of gray level  $r_i$ . The  $n$ th moment of  $r$  about its mean is defined as

$$\mu_n(r) = \sum_{i=0}^{L-1} (r_i - m)^n p(r_i) \quad (3.3-18)$$

where  $m$  is the mean value of  $r$  (its average gray level):

$$m = \sum_{i=0}^{L-1} r_i p(r_i). \quad (3.3-19)$$

It follows from Eqs. (3.3-18) and (3.3-19) that  $\mu_0 = 1$  and  $\mu_1 = 0$ . The second moment is given by

$$\mu_2(r) = \sum_{i=0}^{L-1} (r_i - m)^2 p(r_i). \quad (3.3-20)$$

We recognize this expression as the variance of  $r$ , which is denoted conventionally by  $\sigma^2(r)$ . The standard deviation is defined simply as the square root of the variance. We will revisit moments in Chapter 11 in connection with image description. In terms of enhancement, however, we are interested primarily in the mean, which is a measure of average gray level in an image, and the variance (or standard deviation), which is a measure of average contrast.

We consider two uses of the mean and variance for enhancement purposes. The *global* mean and variance are measured over an entire image and are useful primarily for gross adjustments of overall intensity and contrast. A much more powerful use of these two measures is in local enhancement, where the *local* mean and variance are used as the basis for making changes that depend on image characteristics in a predefined region about each pixel in the image.

Let  $(x, y)$  be the coordinates of a pixel in an image, and let  $S_{xy}$  denote a neighborhood (subimage) of specified size, centered at  $(x, y)$ . From Eq. (3.3-19) the mean value  $m_{S_{xy}}$  of the pixels in  $S_{xy}$  can be computed using the expression

$$m_{S_{xy}} = \sum_{(s,t) \in S_{xy}} r_{s,t} p(r_{s,t}) \quad (3.3-21)$$

where  $r_{s,t}$  is the gray level at coordinates  $(s, t)$  in the neighborhood, and  $p(r_{s,t})$  is the neighborhood normalized histogram component corresponding to that value of gray level. Similarly, from Eq. (3.3-20), the gray-level variance of the pixels in region  $S_{xy}$  is given by

$$\sigma_{S_{xy}}^2 = \sum_{(s,t) \in S_{xy}} [r_{s,t} - m_{S_{xy}}]^2 p(r_{s,t}). \quad (3.3-22)$$

The local mean is a measure of average gray level in neighborhood  $S_{xy}$ , and the variance (or standard deviation) is a measure of contrast in that neighborhood.

An important aspect of image processing using the local mean and variance is the flexibility they afford in developing simple, yet powerful enhancement techniques based on statistical measures that have a close, predictable correspondence with image appearance. We illustrate these characteristics by means of an example.

■ Figure 3.24 shows an SEM (scanning electron microscope) image of a tungsten filament wrapped around a support. The filament in the center of the image and its support are quite clear and easy to study. There is another filament structure on the right side of the image, but it is much darker and its size and other features are not as easily discernable. Local enhancement by contrast manipulation is an ideal approach to try on problems such as this, where part of the image is acceptable, but other parts may contain hidden features of interest.

**EXAMPLE 3.6:**  
Enhancement based on local statistics.

In this particular case, the problem is to enhance dark areas while leaving the light area as unchanged as possible since it does not require enhancement. We can use the concepts presented in this section to formulate an enhancement method that can tell the difference between dark and light and, at the same time, is capable of enhancing only the dark areas. A measure of whether an area is relatively light or dark at a point  $(x, y)$  is to compare the local average gray level  $m_{S_{xy}}$  to the average image gray level, called the global mean and denoted  $M_G$ . This latter quantity is obtained by letting  $S$  encompass the entire image. Thus, we have the first element of our enhancement scheme: We will consider the pixel at a point  $(x, y)$  as a candidate for processing if  $m_{S_{xy}} \leq k_0 M_G$ , where  $k_0$  is a positive constant with value less than 1.0. Since we are interested in enhancing areas that have low contrast, we also need a measure to determine whether the contrast of an area makes it a candidate for enhancement. Thus, we will consider the pixel at a point  $(x, y)$  as a candidate for enhancement if  $\sigma_{S_{xy}} \leq k_2 D_G$ , where  $D_G$  is the global standard deviation and  $k_2$  is a positive constant. The value of this constant will be greater than 1.0 if we are interested in enhancing light areas and less than 1.0 for dark areas. Finally, we need to restrict

the lowest values of contrast we are willing to accept, otherwise the procedure would attempt to enhance even constant areas, whose standard deviation is zero. Thus, we also set a lower limit on the local standard deviation by requiring that  $k_1 D_G \leq \sigma_{s_{xy}}$ , with  $k < k_2$ . A pixel at  $(x, y)$  that meets all the conditions for local enhancement is processed simply by multiplying it by a specified constant,  $E$ , to increase (or decrease) the value of its gray level relative to the rest of the image. The values of pixels that do not meet the enhancement conditions are left unchanged.

A summary of the enhancement method is as follows. Let  $f(x, y)$  represent the value of an image pixel at any image coordinates  $(x, y)$ , and let  $g(x, y)$  represent the corresponding enhanced pixel at those coordinates. Then

$$g(x, y) = \begin{cases} E \cdot f(x, y) & \text{if } m_{s_{xy}} \leq k_0 M_G \text{ AND } k_1 D_G \leq \sigma_{s_{xy}} \leq k_2 D_G \\ f(x, y) & \text{otherwise} \end{cases}$$

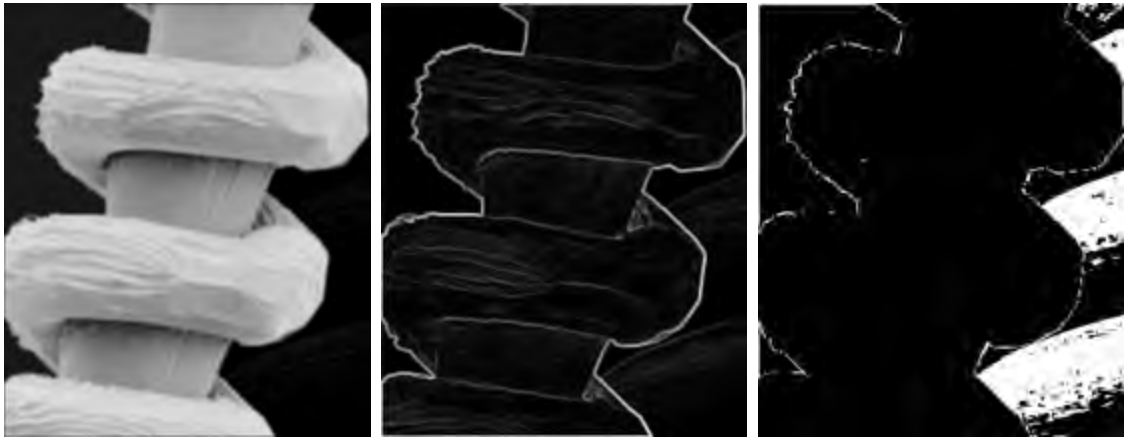
where, as indicated previously,  $E$ ,  $k_0$ ,  $k_1$ , and  $k_2$  are specified parameters;  $M_G$  is the global mean of the input image; and  $D_G$  is its global standard deviation.

Normally, making a successful selection of parameters requires a bit of experimentation to gain familiarity with a given image or class of images. In this case, the following values were selected:  $E = 4.0$ ,  $k_0 = 0.4$ ,  $k_1 = 0.02$ , and  $k_2 = 0.4$ . The relatively low value of 4.0 for  $E$  was chosen so that, when it was multiplied by the levels in the areas being enhanced (which are dark), the result would still tend toward the dark end of the scale, and thus preserve the general visual balance of the image. The value of  $k_0$  was chosen as somewhat less than half the global mean since it is obvious by looking at the image that the areas that require enhancement definitely are dark enough to be below half the global mean. A similar analysis led to the choice of values for  $k_1$  and  $k_2$ . Choosing these constants is not a difficult task in general, but their choice

**FIGURE 3.24** SEM image of a tungsten filament and support, magnified approximately 130 $\times$ . (Original image courtesy of Mr. Michael Shaffer, Department of Geological Sciences, University of Oregon, Eugene).







a b c

**FIGURE 3.25** (a) Image formed from all local means obtained from Fig. 3.24 using Eq. (3.3-21). (b) Image formed from all local standard deviations obtained from Fig. 3.24 using Eq. (3.3-22). (c) Image formed from all multiplication constants used to produce the enhanced image shown in Fig. 3.26.

definitely must be guided by a logical analysis of the enhancement problem at hand. Finally, the choice of size for the local area should be as small as possible in order to preserve detail and keep the computational burden as low as possible. We chose a small ( $3 \times 3$ ) local region.

Figure 3.25(a) shows the values of  $m_{s_{xy}}$  for all values of  $(x, y)$ . Since the value of  $m_{s_{xy}}$  for each  $(x, y)$  is the average of the neighboring pixels in a  $3 \times 3$  area centered at  $(x, y)$ , we expect the result to be similar to the original image, but



**FIGURE 3.26** Enhanced SEM image. Compare with Fig. 3.24. Note in particular the enhanced area on the right, bottom side of the image.

slightly blurred. This indeed is the case in Fig. 3.25(a). Figure 3.25(b) shows an image formed using all the values of  $\sigma_{s_{xy}}$ . Similarly, we can construct an image out the values that multiply  $f(x, y)$  at each coordinate pair  $(x, y)$  to form  $g(x, y)$ . Since the values are either 1 or  $E$ , the image is binary, as shown in Fig. 3.25(c). The dark areas correspond to 1 and the light areas to  $E$ . Thus, any light point in Fig. 3.25(c) signifies a coordinate pair  $(x, y)$  at which the enhancement procedure multiplied  $f(x, y)$  by  $E$  to produce an enhanced pixel. The dark points represent coordinates at which the procedure did not to modify the pixel values.

The enhanced image obtained with the method just described is shown in Fig. 3.26. In comparing this image with the original in Fig. 3.24, we note the obvious detail that has been brought out on the right side of the enhanced image. It is worthwhile to point out that the unenhanced portions of the image (the light areas) were left intact for the most part. We do note the appearance of some small bright dots in the shadow areas where the coil meets the support stem, and around some of the borders between the filament and the background. These are undesirable artifacts created by the enhancement technique. In other words, the points appearing as light dots met the criteria for enhancement and their values were amplified by factor  $E$ . Introduction of artifacts is a definite drawback of a method such as the one just described because of the nonlinear way in which they process an image. The key point here, however, is that the image was enhanced in a most satisfactory way as far as bringing out the desired detail. ■

It is not difficult to imagine the numerous ways in which the example just given could be adapted or extended to other situations in which local enhancement is applicable.

### 3.4 Enhancement Using Arithmetic/Logic Operations

Arithmetic/logic operations involving images are performed on a pixel-by-pixel basis between two or more images (this excludes the logic operation NOT, which is performed on a single image). As an example, subtraction of two images results in a new image whose pixel at coordinates  $(x, y)$  is the difference between the pixels in that same location in the two images being subtracted. Depending on the hardware and/or software being used, the actual mechanics of implementing arithmetic/logic operations can be done sequentially, one pixel at a time, or in parallel, where all operations are performed simultaneously.

Logic operations similarly operate on a pixel-by-pixel basis<sup>†</sup>. We need only be concerned with the ability to implement the AND, OR, and NOT logic operators because these three operators are *functionally complete*. In other words, any other logic operator can be implemented by using only these three basic functions. When dealing with logic operations on gray-scale images, pixel values are processed as strings of binary numbers. For example, performing the NOT operation on a black, 8-bit pixel (a string of eight 0's) produces a white pixel

<sup>†</sup> Recall that, for two binary variables  $a$  and  $b$ :  $a\text{AND}b$  yields 1 only when both  $a$  and  $b$  are 1; otherwise the result is 0. Similarly,  $a\text{OR}b$  is 0 when both variables are 0; otherwise the result is 1. Finally, if  $a$  is 1, NOT ( $a$ ) is 0, and vice versa.



a	b	c
d	e	f

**FIGURE 3.27**

(a) Original image. (b) AND image mask. (c) Result of the AND operation on images (a) and (b). (d) Original image. (e) OR image mask. (f) Result of operation OR on images (d) and (e).

(a string of eight 1's). Intermediate values are processed the same way, changing all 1's to 0's and vice versa. Thus, the NOT logic operator performs the same function as the negative transformation of Eq. (3.2-1). The AND and OR operations are used for *masking*; that is, for selecting subimages in an image, as illustrated in Fig. 3.27. In the AND and OR image masks, light represents a binary 1 and dark represents a binary 0. Masking sometimes is referred to as *region of interest (ROI)* processing. In terms of enhancement, masking is used primarily to isolate an area for processing. This is done to highlight that area and differentiate it from the rest of the image. Logic operations also are used frequently in conjunction with morphological operations, as discussed in Chapter 9.

Of the four arithmetic operations, subtraction and addition (in that order) are the most useful for image enhancement. We consider division of two images simply as multiplication of one image by the reciprocal of the other. Aside from the obvious operation of multiplying an image by a constant to increase its average gray level, image multiplication finds use in enhancement primarily as a masking operation that is more general than the logical masks discussed in the previous paragraph. In other words, multiplication of one image by another can be used to implement gray-level, rather than binary, masks. We give an example in Section 3.8 of how such a masking operation can be a useful tool. In the remainder of this section, we develop and illustrate methods based on subtraction and addition for image enhancement. Other uses of image multiplication are discussed in Chapter 5, in the context of image restoration.

### 3.4.1 Image Subtraction

The difference between two images  $f(x, y)$  and  $h(x, y)$ , expressed as

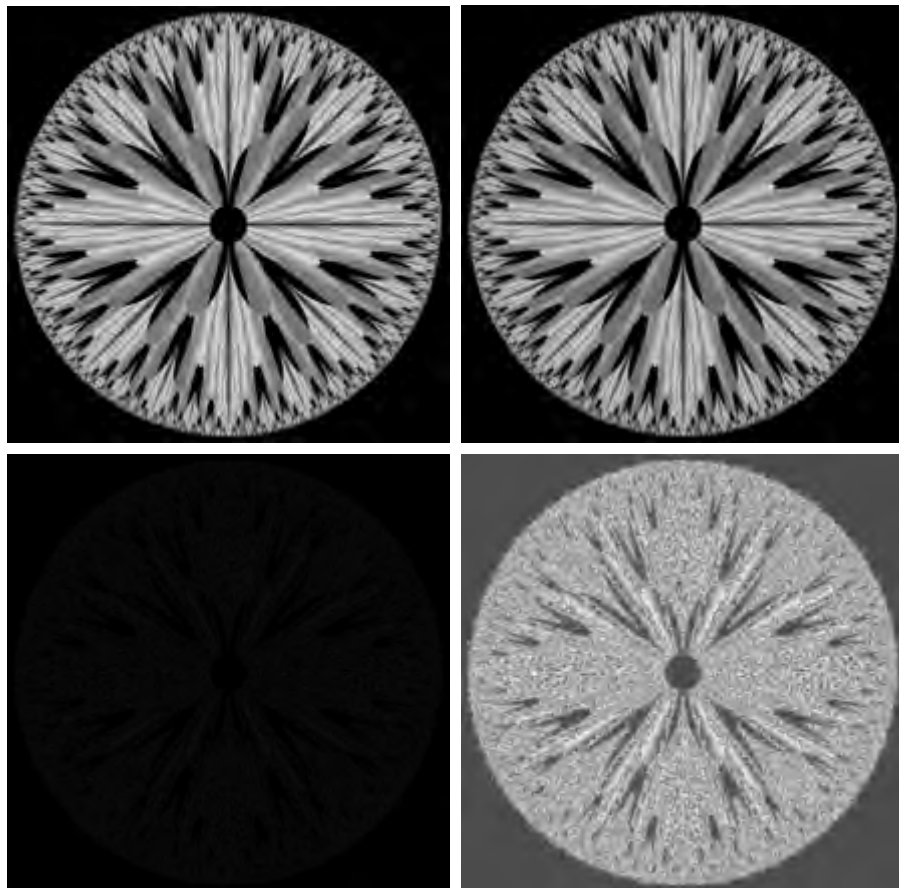
$$g(x, y) = f(x, y) - h(x, y), \quad (3.4-1)$$

is obtained by computing the difference between all pairs of corresponding pixels from  $f$  and  $h$ . The key usefulness of subtraction is the enhancement of *differences* between images. We illustrate this concept by returning briefly to the discussion in Section 3.2.4, where we showed that the higher-order bit planes carry a significant amount of visually relevant detail, while the lower planes contribute more to fine (often imperceptible) detail. Figure 3.28(a) shows the fractal image used earlier to illustrate the concept of bit planes. Figure 3.28(b) shows the result of discarding (setting to zero) the four least significant bit planes of the original image. The images are nearly identical visually, with the exception of a very slight drop in overall contrast due to less variability of the gray-level values in the image of Fig. 3.28(b). The pixel-by-pixel difference between these two images is shown in Fig. 3.28(c). The differences in pixel values are so small that the difference image appears nearly black when displayed on an 8-bit

a b  
c d

**FIGURE 3.28**

(a) Original fractal image.  
(b) Result of setting the four lower-order bit planes to zero.  
(c) Difference between (a) and (b).  
(d) Histogram-equalized difference image.  
(Original image courtesy of Ms. Melissa D. Binde, Swarthmore College, Swarthmore, PA).



display. In order to bring out more detail, we can perform a contrast stretching transformation, such as those discussed in Sections 3.2 or 3.3. We chose histogram equalization, but an appropriate power-law transformation would have done the job also. The result is shown in Fig. 3.28(d). This is a very useful image for evaluating the effect of setting to zero the lower-order planes.

■ One of the most commercially successful and beneficial uses of image subtraction is in the area of medical imaging called *mask mode radiography*. In this case  $h(x, y)$ , the *mask*, is an X-ray image of a region of a patient's body captured by an intensified TV camera (instead of traditional X-ray film) located opposite an X-ray source. The procedure consists of injecting a contrast medium into the patient's bloodstream, taking a series of images of the same anatomical region as  $h(x, y)$ , and subtracting this mask from the series of incoming images after injection of the contrast medium. The net effect of subtracting the mask from each sample in the incoming stream of TV images is that the areas that are different between  $f(x, y)$  and  $h(x, y)$  appear in the output image as enhanced detail. Because images can be captured at TV rates, this procedure in essence gives a movie showing how the contrast medium propagates through the various arteries in the area being observed.

Figure 3.29(a) shows an X-ray image of the top of a patient's head prior to injection of an iodine medium into the bloodstream. The camera yielding this image was positioned above the patient's head, looking down. As a reference point, the bright spot in the lower one-third of the image is the core of the spinal column. Figure 3.29(b) shows the difference between the mask (Fig. 3.29a) and an image taken some time after the medium was introduced into the bloodstream. The bright arterial paths carrying the medium are unmistakably enhanced in Fig. 3.29(b). These arteries appear quite bright because they are not subtracted out (that is, they are not part of the mask image). The overall background is much darker than that in Fig. 3.29(a) because differences between areas of little change yield low values, which in turn appear as dark shades of gray in the difference image. Note, for instance, that the spinal cord, which is bright in Fig. 3.29(a), appears quite dark in Fig. 3.29(b) as a result of subtraction. ■

**EXAMPLE 3.7:**  
Use of image subtraction in mask mode radiography.

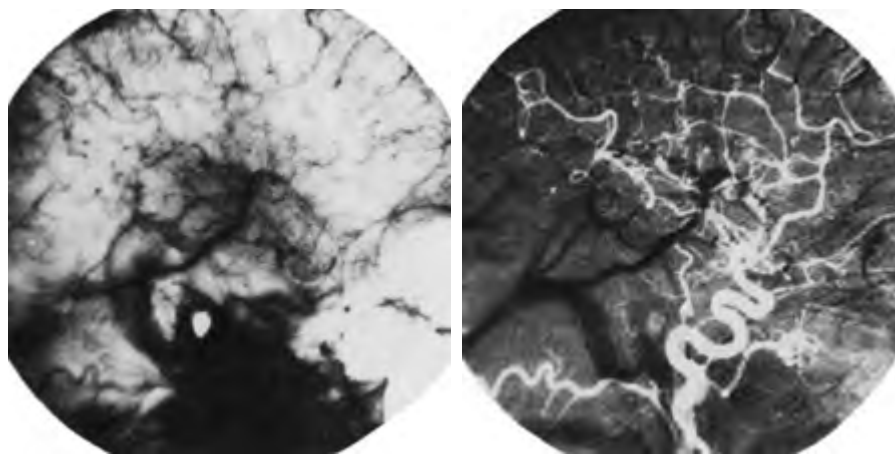


**FIGURE 3.29**  
Enhancement by image subtraction. (a) Mask image. (b) An image (taken after injection of a contrast medium into the bloodstream) with mask subtracted out.

A few comments on implementation are an order before we leave this section. In practice, most images are displayed using 8 bits (even 24-bit color images consists of three separate 8-bit channels). Thus, we expect image values not to be outside the range from 0 to 255. The values in a difference image can range from a minimum of  $-255$  to a maximum of  $255$ , so some sort of scaling is required to display the results. There are two principal ways to scale a difference image. One method is to add  $255$  to every pixel and then divide by  $2$ . It is not guaranteed that the values will cover the entire 8-bit range from  $0$  to  $255$ , but all pixel values definitely will be within this range. This method is fast and simple to implement, but it has the limitations that the full range of the display may not be utilized and, potentially more serious, the truncation inherent in the division by  $2$  will generally cause loss in accuracy.

If more accuracy and full coverage of the 8-bit range are desired, then we can resort to another approach. First, the value of the minimum difference is obtained and its negative added to all the pixels in the difference image (this will create a modified difference image whose minimum values is  $0$ ). Then, all the pixels in the image are scaled to the interval  $[0, 255]$  by multiplying each pixel by the quantity  $255/\text{Max}$ , where  $\text{Max}$  is the maximum pixel value in the modified difference image. It is evident that this approach is considerably more complex and difficult to implement.

Before leaving this section we note also that change detection via image subtraction finds another major application in the area of segmentation, which is the topic of Chapter 10. Basically, segmentation techniques attempt to subdivide an image into regions based on a specified criterion. Image subtraction for segmentation is used when the criterion is “changes.” For instance, in tracking (segmenting) moving vehicles in a sequence of images, subtraction is used to remove all stationary components in an image. What is left should be the moving elements in the image, plus noise.

### 3.4.2 Image Averaging

Consider a noisy image  $g(x, y)$  formed by the addition of noise  $\eta(x, y)$  to an original image  $f(x, y)$ ; that is,

$$g(x, y) = f(x, y) + \eta(x, y) \quad (3.4-2)$$

where the assumption is that at every pair of coordinates  $(x, y)$  the noise is uncorrelated<sup>†</sup> and has zero average value. The objective of the following procedure is to reduce the noise content by adding a set of noisy images,  $\{g_i(x, y)\}$ .

If the noise satisfies the constraints just stated, it can be shown (Problem 3.15) that if an image  $\bar{g}(x, y)$  is formed by averaging  $K$  different noisy images,

$$\bar{g}(x, y) = \frac{1}{K} \sum_{i=1}^K g_i(x, y) \quad (3.4-3)$$

---

<sup>†</sup>Recall that the variance of a random variable  $x$  with mean  $m$  is defined as  $E[(x - m)^2]$ , where  $E\{\cdot\}$  is the expected value of the argument. The covariance of two random variables  $x_i$  and  $x_j$  is defined as  $E[(x_i - m_i)(x_j - m_j)]$ . If the variables are *uncorrelated*, their covariance is  $0$ .

then it follows that

$$E\{\bar{g}(x, y)\} = f(x, y) \quad (3.4-4)$$

and

$$\sigma_{\bar{g}(x, y)}^2 = \frac{1}{K} \sigma_{\eta(x, y)}^2 \quad (3.4-5)$$

where  $E\{\bar{g}(x, y)\}$  is the expected value of  $\bar{g}$ , and  $\sigma_{\bar{g}(x, y)}^2$  and  $\sigma_{\eta(x, y)}^2$  are the variances of  $\bar{g}$  and  $\eta$ , all at coordinates  $(x, y)$ . The standard deviation at any point in the average image is

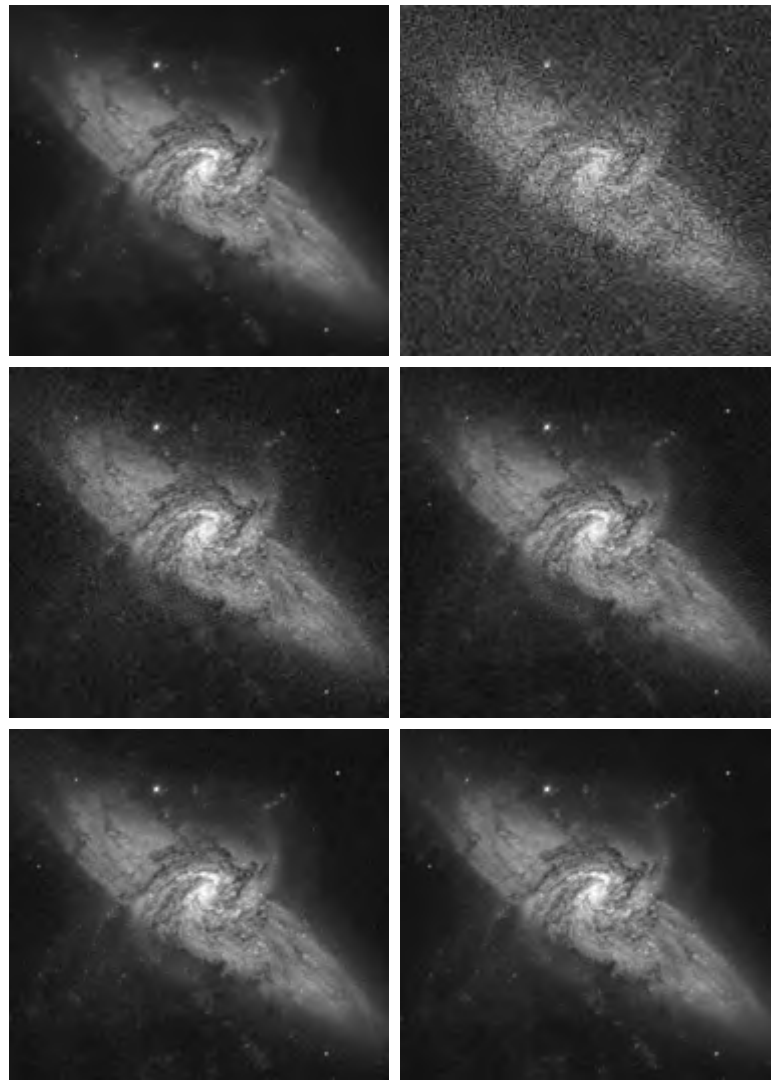
$$\sigma_{\bar{g}(x, y)} = \frac{1}{\sqrt{K}} \sigma_{\eta(x, y)}. \quad (3.4-6)$$

As  $K$  increases, Eqs. (3.4-5) and (3.4-6) indicate that the variability (noise) of the pixel values at each location  $(x, y)$  decreases. Because  $E\{\bar{g}(x, y)\} = f(x, y)$ , this means that  $\bar{g}(x, y)$  approaches  $f(x, y)$  as the number of noisy images used in the averaging process increases. In practice, the images  $g_i(x, y)$  must be registered (aligned) in order to avoid the introduction of blurring and other artifacts in the output image.

■ An important application of image averaging is in the field of astronomy, where imaging with very low light levels is routine, causing sensor noise frequently to render single images virtually useless for analysis. Figure 3.30(a) shows an image of a galaxy pair called NGC 3314, taken by NASA's Hubble Space Telescope with a wide field planetary camera. NGC 3314 lies about 140 million light-years from Earth, in the direction of the southern-hemisphere constellation Hydra. The bright stars forming a pinwheel shape near the center of the front galaxy have formed recently from interstellar gas and dust. Figure 3.30(b) shows the same image, but corrupted by uncorrelated Gaussian noise with zero mean and a standard deviation of 64 gray levels. This image is useless for all practical purposes. Figures 3.30(c) through (f) show the results of averaging 8, 16, 64, and 128 images, respectively. We see that the result obtained with  $K = 128$  is reasonably close to the original in visual appearance.

We can get a better appreciation from Fig. 3.31 for how reduction in the visual appearance of noise takes place as a function of increasing  $K$ . This figure shows the difference images between the original [Fig. 3.30(a)] and each of the averaged images in Figs. 3.30(c) through (f). The histograms corresponding to the difference images are also shown in the figure. As usual, the vertical scale in the histograms represents number of pixels and is in the range  $[0, 2.6 \times 10^4]$ . The horizontal scale represents gray level and is in the range  $[0, 255]$ . Notice in the histograms that the mean and standard deviation of the difference images decrease as  $K$  increases. This is as expected because, according to Eqs. (3.4-3) and (3.4-4), the average image should approach the original as  $K$  increases. We can also see the effect of a decreasing mean in the difference images on the left column of Fig. 3.31, which become darker as the  $K$  increases.

**EXAMPLE 3.8:**  
Noise reduction  
by image  
averaging.

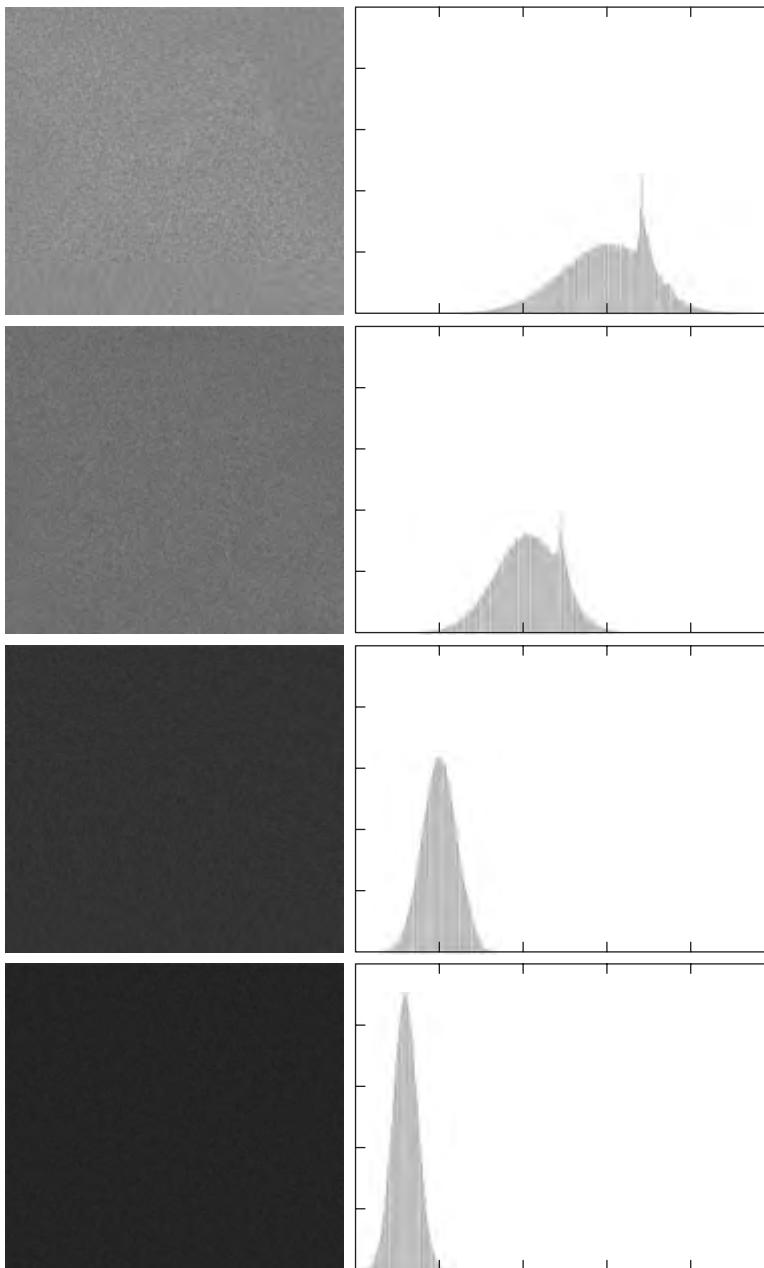


a	b
c	d
e	f

**FIGURE 3.30** (a) Image of Galaxy Pair NGC 3314. (b) Image corrupted by additive Gaussian noise with zero mean and a standard deviation of 64 gray levels. (c)–(f) Results of averaging  $K = 8, 16, 64,$  and  $128$  noisy images. (Original image courtesy of NASA.)

Addition is the discrete formulation of continuous integration. In astronomical observations, a process equivalent to the method just described is to use the integrating capabilities of CCD or similar sensors for noise reduction by observing the same scene over long periods of time. The net effect, however, is analogous to the procedure just discussed. Cooling the sensor further reduces its noise level. ■





**a b**  
**FIGURE 3.31**  
 (a) From top to bottom: Difference images between Fig. 3.30(a) and the four images in Figs. 3.30(c) through (f), respectively. (b) Corresponding histograms.

As in the case of image subtraction, adding two or more 8-bit images requires special care when it comes to displaying the result on an 8-bit display. The values in the sum of  $K$ , 8-bit images can range from 0 to  $255 \times K$ . Scaling back to 8 bits in this case consists simply of dividing the result by  $K$ . Naturally, some accuracy will be lost in the process, but this is unavoidable if the display has to be limited to 8 bits.

It is possible in some implementations of image averaging to have negative values when noise is added to an image. In fact, in the example just given, this was precisely the case because Gaussian random variables with zero mean and nonzero variance have negative as well as positive values. The images in the example were scaled using the second scaling method discussed at the end of the previous section. That is, the minimum value in a given average image was obtained and its negative was added to the image. Then all the pixels in the modified image were scaled to the range  $[0, 255]$  by multiplying each pixel in the modified image by the quantity  $255/\text{Max}$ , where  $\text{Max}$  was the maximum pixel value in that image.

### 3.5 Basics of Spatial Filtering

As mentioned in Section 3.1, some neighborhood operations work with the values of the image pixels in the neighborhood *and* the corresponding values of a subimage that has the same dimensions as the neighborhood. The subimage is called a *filter*, *mask*, *kernel*, *template*, or *window*, with the first three terms being the most prevalent terminology. The values in a filter subimage are referred to as *coefficients*, rather than pixels.

The concept of filtering has its roots in the use of the Fourier transform for signal processing in the so-called *frequency domain*. This topic is discussed in more detail in Chapter 4. In the present chapter, we are interested in filtering operations that are performed directly on the pixels of an image. We use the term *spatial filtering* to differentiate this type of process from the more traditional frequency domain filtering.

The mechanics of spatial filtering are illustrated in Fig. 3.32. The process consists simply of moving the filter mask from point to point in an image. At each point  $(x, y)$ , the *response* of the filter at that point is calculated using a predefined relationship. For *linear* spatial filtering (see Section 2.6 regarding linearity), the response is given by a sum of products of the filter coefficients and the corresponding image pixels in the area spanned by the filter mask. For the  $3 \times 3$  mask shown in Fig. 3.32, the result (or response),  $R$ , of linear filtering with the filter mask at a point  $(x, y)$  in the image is

$$R = w(-1, -1)f(x - 1, y - 1) + w(-1, 0)f(x - 1, y) + \cdots \\ + w(0, 0)f(x, y) + \cdots + w(1, 0)f(x + 1, y) + w(1, 1)f(x + 1, y + 1),$$

which we see is the sum of products of the mask coefficients with the corresponding pixels directly under the mask. Note in particular that the coefficient  $w(0, 0)$  coincides with image value  $f(x, y)$ , indicating that the mask is centered at  $(x, y)$  when the computation of the sum of products takes place. For a mask of size  $m \times n$ , we assume that  $m = 2a + 1$  and  $n = 2b + 1$ , where  $a$  and  $b$  are nonnegative integers. All this says is that our focus in the following discussion will be on masks of *odd* sizes, with the smallest meaningful size being  $3 \times 3$  (we exclude from our discussion the trivial case of a  $1 \times 1$  mask).